CHAPTER 3

Evaluation of Atmospheric Loss Processes

Lead Authors:
James B. Burkholder
Wahid Mellouki

Co-Authors:
Eric L. Fleming
Christian George
Dwayne E. Heard
Charles H. Jackman
Michael J. Kurylo
Vladimir L. Orkin
William H. Swartz
Timothy J. Wallington

CHAPTER 3

Evaluation of Atmospheric Loss Processes

Contents

SUPPLEMENTARY MATERIAL

The Chapter 3 supplements are not included in the printed report.

The digital version of the report, with supplements, is available at:

http://www.sparc-climate.org/publications/sparc-reports/sparc-report-no6/

3.0 Summary

- Hydroxyl radical (OH), electronically excited atomic oxygen ($O(^1D)$), and atomic chlorine (Cl) reaction-rate coefficient data were evaluated and the estimated uncertainties in the recommended parameters reduced, in general, from those currently recommended in the NASA/Jet Propulsion Laboratory (JPL) and International Union of Pure and Applied Chemistry (IUPAC) kinetic and photochemical data evaluations.
- New studies of several $O(^1D)$ reaction-rate coefficients, reaction yields, and their temperature dependences provided data needed to reduce uncertainties in calculated lifetimes.
- Lyman-α (121.567 nm) absorption cross-section recommendations are provided and uncertainties estimated. Lyman-α photolysis is shown to be a dominant mesospheric loss process, but makes only a minor contribution to the total global atmospheric lifetimes for the molecules included in this report.
- Ultraviolet (UV) absorption cross-section data were evaluated and new cross-section parameterizations recommended for CCl_4 (carbon tetrachloride), CF_2Br_2 (Halon-1202), CF_2ClBr (Halon-1211), CF_2BrCF_2Br (Halon-2402), and NF_3 (nitrogen trifluoride). In addition, systematic errors in the UV spectrum parameterizations for $CFCl_3$ (CFC-11), CF_2Cl_2 (CFC-12), $CFCl_2CF_2Cl$ (CFC-113), CF_2ClCF_2Cl (CFC-114), CH_3CCl_3, CH_3Cl, and CHF_2Cl (HCFC-22) given in literature and quoted in NASA/JPL (JPL10-6) from the original literature are corrected here. Uncertainties in absorption cross-sections and their temperature dependence are estimated for 5 key photolysis wavelength regions.
- Two-dimensional (2-D) atmospheric model calculations were used to quantify the fractional contribution of the OH, $O(^1D)$, and Cl reactive losses as well as photolytic loss to the global annually averaged local and overall lifetimes for each of the molecules included in this report. For hydrogen containing molecules, loss due to the OH reaction is dominant (>90%). The dominant loss process for the chlorofluorocarbons (CFCs), CCl_4, N_2O (nitrous oxide), CF_3Br (Halon-1301), and NF_3 is photolysis primarily in the stratosphere in the 190-230 nanometer (nm) wavelength region. For CF_2Br_2 (Halon-1202), CF_2BrCl (Halon-1211), and CF_2BrCF_2Br (Halon-2402) photolysis in the 190-230 and >286 nm regions contribute to their atmospheric removal. Loss due to $O(^1D)$ atom reaction, which is primarily a stratospheric loss process, is generally of secondary importance. Loss due to Cl atom reaction is minor (<1.5% for CH_4 (methane) and <0.5% for the other molecules in this study).
- 2-D atmospheric model calculations showed that existing uncertainties in kinetic and photochemical parameters contribute substantial uncertainty to calculated atmospheric lifetimes. The estimated uncertainties given in the present Stratospheric Processes and Their Role in Climate (SPARC) parameter recommendations, in general, lead to a reduction in the range of calculated lifetimes from those calculated using the NASA/JPL (JPL10-6) recommended kinetic parameters. For $CFCl_3$ (CFC-11), CF_2Cl_2 (CFC-12), CCl_4, and N_2O the range in calculated lifetimes is between 5 and 10%, while for CH_3CCl_3 (methyl chloroform) and CHF_2Cl (HCFC-22) it is ~20%.

3.1 Introduction

An evaluation of the atmospheric lifetime of a trace gas requires a thorough understanding of its chemical loss processes. In this chapter, a comprehensive evaluation of the available experimental data for the key atmospheric removal processes, including results of a thorough uncertainty analysis, is presented. This chapter includes an evaluation of the OH, $O(^1D)$, and Cl gas-phase reaction-rate coefficients, *k*, and their temperature dependences, and of the vacuum ultraviolet/ultraviolet (VUV/UV) absorption spectra (photodissociation) for each of the molecules included in this report. Atmospheric lifetimes were evaluated using 2-D atmospheric model calculations, based on the recommendations given in the NASA/JPL evaluation (Sander *et al.*, 2011) and those presented here. The range in the calculated lifetimes determined from the ranges of uncertainties in the chemical loss parameters (reaction and photolysis) are also presented.

The recommendations given in this assessment benefit significantly from the activities of two long-term independent international photochemistry and kinetics data evaluation panels: the NASA/JPL Panel for Data Evaluation, "Chemical Kinetics and Photochemical Data for Use in Atmospheric Studies" (Sander *et al.*, 2011) (herein referred to as JPL10-6), and the IUPAC Subcommittee for Gas Kinetic Data Evaluation (Atkinson *et al.*, 2008) (herein referred to as IUPAC). In addition, the Max Planck Institute (MPI) for Chemistry spectral data compilation (Keller-Rudek and Moortgat) was a useful resource in the photolysis data evaluation.

Hydrochlorofluorocarbons (HCFCs) and hydrofluorocarbons (HFCs) are, in most cases, primarily removed from the atmosphere by reaction with the OH radical. There are relatively few new studies since JPL10-6 and a focus of the present evaluation of the OH kinetics was on the recommended uncertainties in the kinetic parameters. The $O(^1D)$ reaction, which is primarily a stratospheric loss process, evaluation includes studies by Feierabend *et al.* (2010), Baasandorj *et al.* (2011; 2012; 2013), and Nilsson *et al.* (2012) that provide additional rate-coefficient and product-yield data that were not available for the JPL10-6 evaluation. The results from these studies combined with previous works have enabled a refinement of the rate coefficients, product yields, and reaction yields as well as a reduction in the recommended uncertainties for a number of reactions. While Cl atom reaction represents a minor loss process for the molecules considered here, the present evaluation has revised several kinetic recommendations and estimated uncertainty parameters. Gas-phase reactions with other atmospheric oxidants, such as O_3 (ozone) and NO_3 (nitrogen trioxide), are expected to be negligible for the molecules included in this report and are not considered further.

Photodissociation is an important loss process for N_2O and NF_3 and for the chlorofluorocarbons (CFCs), hydrochlorofluorocarbons (HCFCs), and fluorochlorobromocarbons (Halons) included in this report. CFCs and HCFCs are photodissociated by UV radiation primarily in the stratosphere, while Halons are photodissociated in the troposphere and stratosphere. Absorption cross sections at the hydrogen Lyman-α wavelength (121.567 nm) were evaluated and photolysis at this wavelength was shown to be a minor loss process in terms of the total global atmosphere in nearly all cases; Lyman-α is the predominate source of photodissociation radiation in the VUV region. Since the JPL10-6 evaluation was released, Papanastasiou *et al.* (2013) reported cross-section data for CF_2Br_2 (Halon-1202), CF_2ClBr (Halon-1211), and CF_2BrCF_2Br (Halon-2402) at wavelengths $\geq$300 nm and Papadimitriou *et al.* (2013) reported NF_3 UV absorption cross-section data and its temperature dependence. The results from these studies have enabled a significant reduction of the uncertainties in the photolysis lifetimes of these molecules. In addition, improved UV absorption cross-section

parameterizations for $CFCl_3$ (CFC-11), CF_2Cl_2 (CFC-12), $CFCl_2CF_2Cl$ (CFC-113), CF_2ClCF_2Cl (CFC-114), CH_3CCl_3, CH_3Cl, and CHF_2Cl (HCFC-22) over those reported in the literature and quoted in JPL10-6 from the original literature are provided in the supplementary material.

Data evaluation is not an exact science and does not conform to a set of rules governing the process. However, consideration of uncertainties in the kinetic and photochemical parameters used in atmospheric models plays a key role in determining the reliability/uncertainty of the model results. Quite often the cause of differences in experimental results from various laboratories cannot be determined with confidence and making recommendations for the uncertainties is often more difficult to derive than for the parameters themselves. In many cases, the investigators only suggest possible qualitative reasons for disagreements among datasets. Thus, data evaluators necessarily consider a variety of factors in assigning a recommendation including factors such as the chemical complexity of the system, sensitivities and shortcomings of the experimental techniques employed, similarities or trends in reactivity, and the level of agreement among studies using different techniques. The rate-coefficient uncertainties presented in this evaluation follow the formalism given in JPL10-6

$$f(\mathrm{T}) = f(298\ \mathrm{K}) \exp\left(\left|g\left(\frac{1}{\mathrm{T}} - \frac{1}{298}\right)\right|\right)$$

where $f(\mathrm{T})$ is an uncertainty factor for $k(\mathrm{T})$, $f(298\ \mathrm{K})$ is the 1σ estimated uncertainty factor for the room-temperature rate coefficient, $k(298\ \mathrm{K})$, and g is a parameter used to describe the increase in uncertainty at temperatures other than 298 K. An upper and lower bound of the rate coefficient at any temperature can be obtained by multiplying or dividing the recommended value, $k(\mathrm{T})$, by the factor $f(\mathrm{T})$. The 2σ uncertainty is given by $f(\mathrm{T})^2$.

The uncertainty recommendations given in the past JPL10-6 and IUPAC evaluations are often rather conservative in that they were chosen, in many cases, to cover the full range of the available experimental data even including results that were not used in quantifying the recommended kinetic parameters. In the present evaluation, the most stringent uncertainty limits (at the 2σ uncertainty level) that can be justified by the available experimental data are reported. In cases where the experimental data did not extend to the lowest temperatures representative of the upper troposphere and lower stratosphere, the uncertainty recommendations were based on a comparison with similar compounds for which studies by multiple investigators or using different experimental techniques did extend to lower temperatures.

An extensive evaluation of the uncertainties in the photochemical data, absorption cross sections, and their temperature dependences, an issue that has not been comprehensively addressed in previous JPL or IUPAC data evaluations, is reported here. The cross-section uncertainties were estimated by comparing the agreement among multiple experimental datasets, whenever possible. Where experimental data do not exist for a compound, e.g., Lyman-α cross sections, cross sections were estimated based on trends observed for similar compounds and relatively conservative uncertainties were assigned. Details of the evaluation for each compound are provided in the supplementary material for this chapter.

Overall, the uncertainty in an atmospheric loss process, for even the most highly studied compounds, is typically >10% and, in many cases, the cumulative uncertainties of the most important loss processes are greater. The NASA/Goddard Space Flight Center (GSFC) two-

dimensional (2-D) coupled chemistry-radiation-dynamics model (Fleming *et al.*, 2011) was used to evaluate the impact of the kinetic and photochemical recommendations and their uncertainties on atmospheric lifetimes. Model calculations of lifetimes and uncertainties are discussed in Section 3.5.

Section 3.6 considers the sensitivity of the calculated lifetimes to the uncertainty in the O_2 and O_3 UV absorption cross sections used in the model calculations. Uncertainty in the O_2 and O_3 cross sections represent a potential uncertainty in the calculated lifetimes via their impact on: (1) the ozone concentration, and (2) the incident solar UV radiation throughout the atmosphere. An evaluation of the 2σ lifetime uncertainty for the species primarily removed in the stratosphere is presented.

Supplemental material for this chapter includes (1) a comprehensive graphical analysis of the available OH, $O(^1D)$, and Cl atom kinetic data, (2) summaries of the available photochemical data and the basis for the recommendations given here, and (3) a graphical summary of the 2-D model results obtained using kinetic and photochemical input parameters from the JPL10-6 data evaluation and the recommendations given here for each of the molecules included in this report.

3.2 Gas-Phase Reactive Loss Processes

Reaction-rate coefficients, $k(T)$, for the OH radical, $O(^1D)$ atom, and Cl atom reactions were parameterized using an Arrhenius expression where $k(T) = A \exp(-E/RT)$ and the pre-exponential, A, and activation energy, E, parameters were taken as variables in the fitting of the experimental data. Figure 3.1 shows an Arrhenius plot, $\ln(k(T))$ vs. $1/T$, for the OH + CHF_2Cl (HCFC-22) reaction (Arrhenius plots are provide in the supplementary material for all the compounds and reactions). Over the temperature range most relevant for atmospheric chemistry, 200 to 300 K, the Arrhenius expression reproduces the experimental data to within the measurement precision, although over a broader temperature range non-Arrhenius behavior (curvature) is observed in some cases, e.g., the Cl and OH reactions with CH_4. The OH + CHF_2Cl reaction is an example where the available experimental data do not cover the complete temperature range applicable for atmospheric chemical processes. In these cases, the higher temperature data were used to extrapolate, using the fitted Arrhenius expression, to lower temperatures. The estimated uncertainty in the extrapolated low-temperature rate-coefficient values was increased, as shown in Figure 3.1, to reflect the increased uncertainties associated with such an extrapolation. The rate-coefficient recommendations for the OH radical, $O(^1D)$ atom, and Cl atom reactions given here are based on a comprehensive evaluation of all available laboratory data. In cases where data do not exist, best estimates for the rate-coefficient parameters are based on the recommendations for similar compounds.

3.2.1 OH Radical Chemistry

While a thorough examination of the OH kinetic data available for every molecule was conducted, particular attention was paid to those molecules for which new data have appeared since the latest data panel evaluations, new insights into chemical mechanisms now exist, or differences between the JPL10-6 and IUPAC recommendations exceed the combined recommended uncertainty limits. The present recommendations are given in Table 3.1. The recommendations do not differ appreciably from those given in JPL10-6 or IUPAC, and details of the evaluation are provided in the footnotes of Table 3.1. The uncertainty parameters given in Table 3.1 are, however, typically smaller than those reported in the JPL10-6 and IUPAC evaluations.

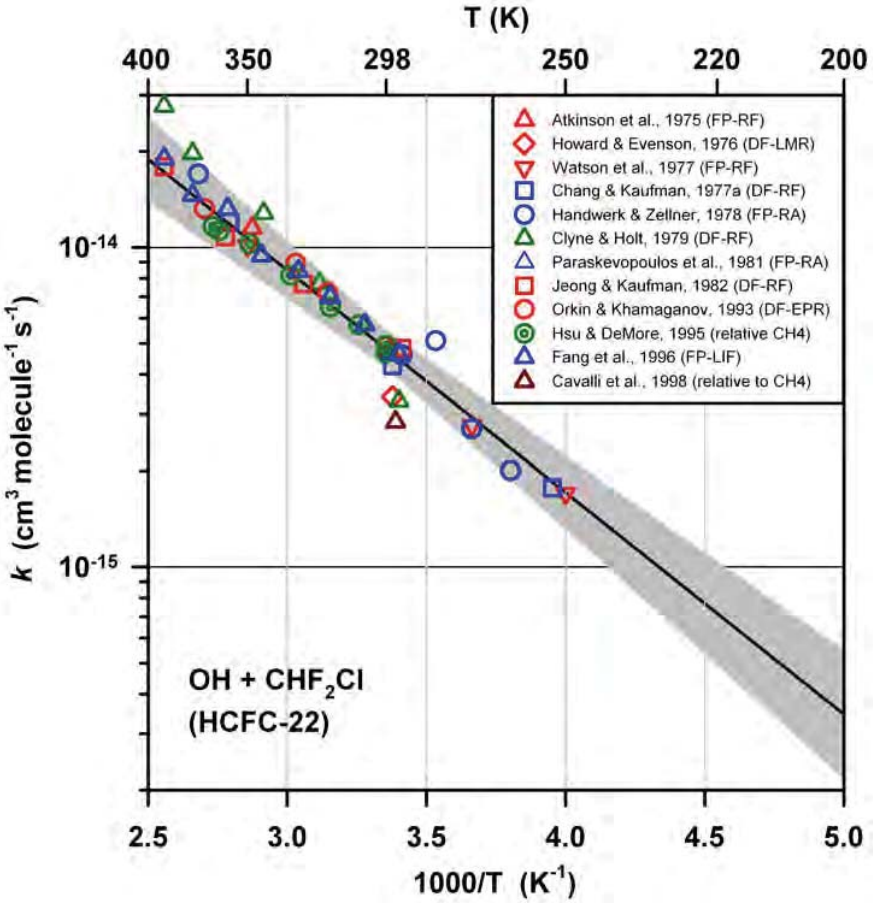

Figure 3.1. Arrhenius plot for the OH + CHF_2Cl (HCFC-22) reaction including all available experimental data (see legend) over the temperature range 200 to 400 K. The solid line is the recommended rate coefficient for use in atmospheric models (see Table 3.1). The gray shaded region represents the estimated 2-σ uncertainty range in k(T) from the present evaluation. Note that there are no experimental data currently available for this reaction below ~250 K and the estimated uncertainties in the extrapolated Arrhenius expression (g factor) are such that the uncertainty in this region is greater.

The recommended kinetic parameters for CH_3CCl_3, CH_3CFCl_2 (HCFC-141b), CH_3CF_2Cl (HCFC-142b), CHF_3 (HFC-23), CH_2F_2 (HFC-32), CHF_2CF_3 (HFC-125), CH_3CHF_2 (HFC-152a), and $CHF_2CH_2CF_3$ (HFC-245fa) are unchanged from those given in JPL10-6. However, the uncertainty recommendations have been reduced in most cases. Minor changes to the JPL10-6 recommendations were made for CH_3Cl, CHF_2Cl (HCFC-22) (see Figure 3.1), CH_2FCF_3 (HFC-134a), and CH_3CF_3 (HFC-143a), based on slight differences in the way that the multiple experimental datasets were combined for fitting. For example, care was taken to not unduly weight a particular study in which multiple data points were reported at a given temperature over those studies that averaged data prior to reporting. For CH_3Br (methyl bromide) and CF_3CHFCF_3 (HFC-227ea), the present recommendations differ more appreciably from those given in JPL10-6 and IUPAC. The difference for CH_3Br stems from the decision to base the temperature dependence on the study by Mellouki *et al.* (1992), rather than on a combined fit to the slightly more scattered data from three other studies that did not extend to as low a temperature (see footnote in Table 3.1). For HFC-227ea, an improved fit of the multiple datasets, which exhibited slight systematic differences, but similar temperature dependences, was made. More specifically, all of the datasets were

normalized to a common value of the rate coefficient at room temperature prior to fitting, thereby reducing biases in the obtained temperature dependence (see supplement). For CH_4, the recommended Arrhenius parameters were taken from the IUPAC evaluation (see supplement).

The rate-coefficient upper-limit recommendations for the fully halogenated species $CFCl_3$ (CFC-11), CF_2Cl_2 (CFC-12), $CF_2ClCFCl_2$ (CFC-113), CF_2ClCF_2Cl (CFC-114), CF_3CF_2Cl (CFC-115), and CCl_4, which are considered as non-reactive towards the OH radical because the abstraction reactions are endothermic, have been reduced by more than an order of magnitude from the upper limits given in JPL10-6 and IUPAC. For CFC-11, CFC-12, and CCl_4, the reaction endothermicities have been taken as lower-limits of the reaction activation energies, *E*. The *E*/R lower-limits have been combined with an estimated upper limit for the Arrhenius *A* factor, based on the largest *A* factor observed in any experimental study of OH + halocarbon reactions. This method of analysis provides a more representative/realistic upper limit for these reaction-rate coefficients for use in atmospheric models. The recommended upper limits are considerably lower than those resulting from actual laboratory studies that are limited by the capabilities of the experimental techniques. For CFC-113, CFC-114, and CFC-115 for which thermochemical data for the possible reaction products are not available, the rate-coefficient recommendation for CCl_4 was taken as an upper limit; the upper-limit recommended for CCl_4 is the highest among the fully halogenated compounds not containing bromine (Br) and having known thermochemistry. As shown in Section 3.5, the estimated rate coefficients for these reactions result in a negligible contribution to the molecules' atmospheric lifetimes.

3.2.2 $O(^1D)$ Atom Chemistry

$O(^1D)$ reactions are complex with several possible exothermic reaction pathways, which include (1) collisional (physical) quenching of $O(^1D)$ to ground state oxygen atoms, $O(^3P)$, (2) abstraction or addition-elimination, and (3) reactive quenching to form $O(^3P)$ and products other than the reactant, including stable and radical species. Although some laboratory kinetic studies have directly observed the temporal profile of $O(^1D)$ atoms using absorption (Heidner and Husain, 1973), laser-induced fluorescence (Blitz *et al.*, 2004), or emission spectroscopy (Davidson *et al.*, 1978), the majority of measurements have utilized indirect methods. The indirect methods used include (1) detection of $O(^3P)$ by atomic resonance absorption (Amimoto *et al.*, 1978) or fluorescence (Wine and Ravishankara, 1981), (2) a competitive reaction technique in which the detection of OH following the reaction of $O(^1D)$ with an atomic hydrogen donor molecule is used (Baasandorj *et al.*, 2011, 2012, 2013; Blitz *et al.*, 2004; Vranckx *et al.*, 2008), and (3) CH radical chemiluminescence following the reaction of $O(^1D)$ with the ethynyl radical (C_2H) (Vranckx *et al.*, 2008). Some studies have also used relative-rate measurements for the determination of reactive-rate coefficients (Baasandorj *et al.*, 2012, 2013; Nilsson *et al.*, 2012; Force and Wiesenfeld, 1981; Green and Wayne, 1976/77), which is critically important to determining the loss of the molecular reactant in the $O(^1D)$ reaction.

Product yields at room temperature have been determined for the majority of the reactions included in this report, for example: ClO (chlorine monoxide) radical yields for the CFC reactions and other chlorine containing reactants (Baasandorj *et al.*, 2011; Feierabend *et al.*, 2010), OH radical yields for the CH_4 reaction and other hydrogen containing reactants (Vranckx *et al.*, 2008), BrO (bromine monoxide) radical yields for several bromine containing reactants including CF_3Br, CF_2ClBr, and CH_3Br (Cronkhite and Wine, 1998), and the NO (nitric oxide) yield in the N_2O reaction (Greenblatt and Ravishankara, 1990). Highly

precise measurements of the $O(^3P)$ yield for several $O(^1D)$ reactions were determined using a CH radical chemiluminescence method (Vranckx *et al.*, 2008).

Recommended overall rate coefficients (i.e., $O(^1D)$ loss), reaction yields, and estimated uncertainties for all of the molecules included in this report are given in Table 3.2, with the footnotes and supplementary material providing details for the recommendations. The recommendations for the overall rate coefficients, in most cases, do not differ appreciably from JPL10-6, although the uncertainty parameters given in Table 3.2 are typically reduced as a result of considering studies that became available after the JPL10-6 evaluation was finalized. In particular, recent studies that included measurements over a range of temperatures enabled significant reductions in the estimated rate-coefficient uncertainties (*g* factor). In general, over the atmospherically relevant temperature range, there is only a weak, if any, temperature dependence for the $O(^1D)$ reaction-rate coefficients as shown in Figure 3.2 for the $O(^1D) + CHF_2Cl$ (HCFC-22) reaction.

The reaction yields reported in Table 3.2 are in some cases appreciably different from JPL10-6. The uncertainties in the reaction yields are, in general, reduced from those reported in JPL10-6 owing to the results from recent studies. Consideration of results from the studies of Feierabend *et al.* (2010) and Baasandorj *et al.* (2011; 2012; 2013) for CFC-11, CFC-12, CCl_4, HCFC-22, CFC-113, CFC-115, HFC-143a, HFC-23, CFC-114, HCFC-142b, HFC-125, HFC-227ea, and NF_3 (nitrogen trifluoride), which became available after the JPL10-6 evaluation was finalized, have resulted in revisions to the recommendations from those given in JPL10-6. An average of the kinetic results from Matsumi *et al.* (1993) and Force and Wiesenfeld (1981) for CH_3Cl and the reactive-rate coefficient for CH_3CCl_3 reported by Nilsson *et al.* (2012), which were not included in JPL10-6, are recommended here. The recommendations that are revised from JPL10-6 are summarized briefly below.

The kinetic results from the Baasandorj *et al.* (2013) study are consistent with the JPL10-6 recommendation for CFC-11 and HCFC-22, but enabled a reduction in the estimated rate coefficients and their temperature-dependence uncertainty. For CFC-12, the recommended rate coefficient is slightly greater than the JPL10-6 recommendation and the reported small negative temperature dependence is recommended. On the basis of the Feierabend *et al.* (2010) study, the recommended ClO radical yields for the CFC-11, CFC-12, and CCl_4 reactions are ~10% lower than given in JPL10-6.

The recommended kinetic values for the CFC-113, CFC-115, HFC-143a, and HFC-23 reactions given here reflect the results from recent studies and differ from those given in JPL10-6. On the basis of the Baasandorj *et al.* (2011) study, the recommended ClO yield for CFC-113 is lower than given in JPL10-6.

The rate coefficients and ClO yield for the CFC-114 reaction are greater than given in JPL10-6. For HCFC-142b and HFC-125, the recent Baasandorj *et al.* (2013) study provided temperature-dependent data, which results in a reduced estimated rate coefficient and temperature-dependence uncertainty. HFC-227ea and HFC-245fa were not evaluated by JPL10-6. The kinetic parameters from Baasandorj *et al.* (2013) for the HFC-227ea reaction, which displays a weak negative temperature dependence, are recommended. For the HFC-245fa reaction, the rate coefficient and reaction yield were estimated. On the basis of the results from Zhao *et al.* (2010) and Baasandorj *et al.* (2012), a reactive yield of 0.93 was recommended for the NF_3 reaction.

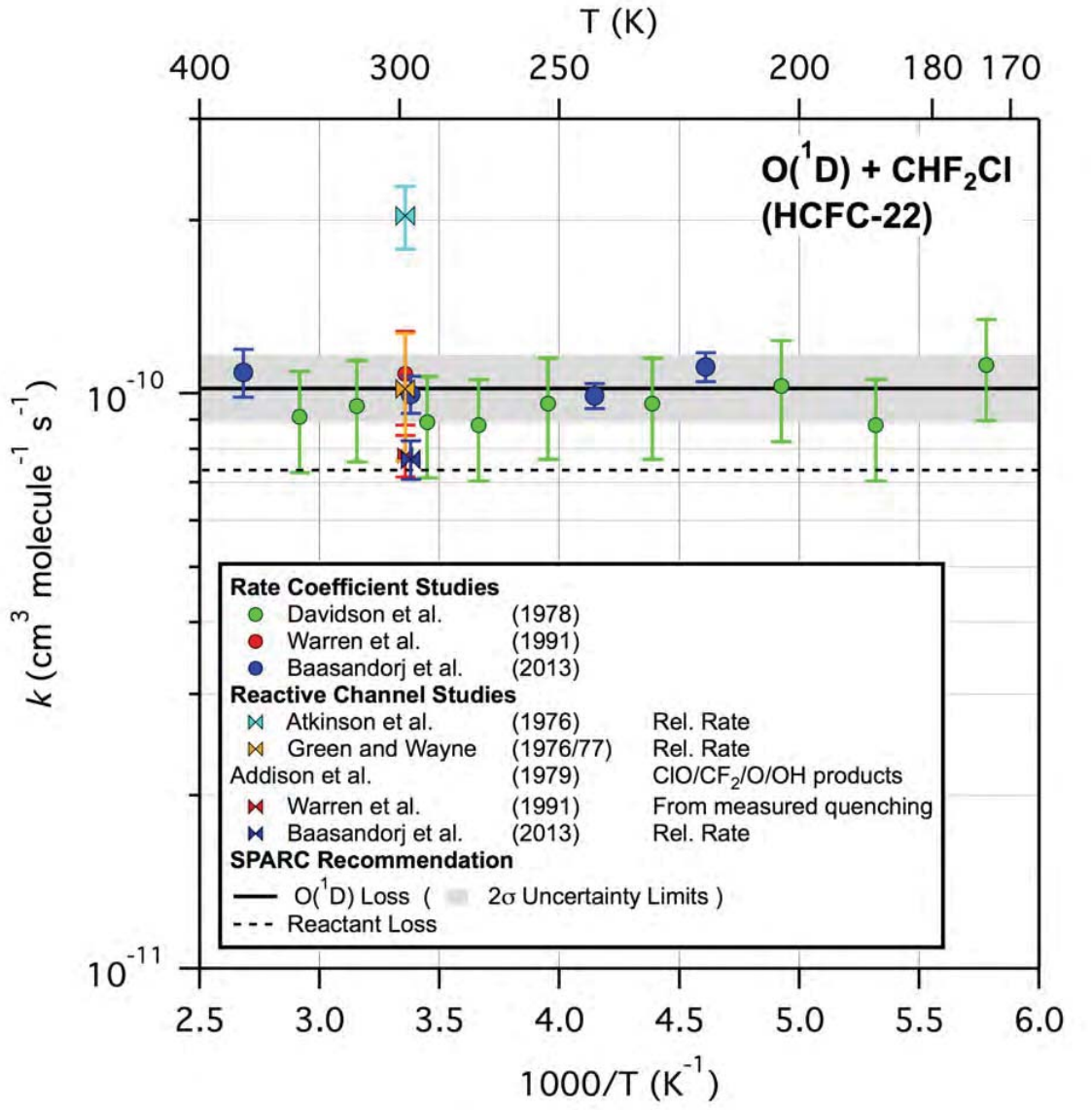

Figure 3.2. Arrhenius plot for the $O(^1D)$ + CHF_2Cl (HCFC-22) reaction including all available experimental total and reactive-rate coefficient data (see legend). The product yield data from the Addison *et al*. (1979) study are not included in the figure. The solid and dashed lines are the total and reactive-rate coefficient recommendations, respectively, from the present evaluation and the shaded region represents the 2σ range from estimated uncertainty in the total rate coefficient.

3.2.3 Cl Atom Chemistry

Reaction-rate coefficient and estimated uncertainty recommendations for the Cl atom reactions are given in Table 3.3, with the footnotes of Table 3.3 providing the details for the recommendations. The recommended kinetic parameters, in most cases, do not differ appreciably from those given in IUPAC and JPL10-6. For compounds with rate coefficients $>10^{-14}$ cm^3 $molecule^{-1}$ s^{-1} at 298 K, there is good agreement, typically within a few percent, between the recommendations from the IUPAC and JPL10-6 data panels. For compounds with rate coefficients $<10^{-14}$ cm^3 $molecule^{-1}$ s^{-1} at 298 K, there are, in some cases, significant

differences between the IUPAC and JPL10-6 recommendations, e.g., ~40% for CF_3CH_3 (HFC-143a) at 220 K. The uncertainty factors given in Table 3.3 are based on the available experimental data as described in the footnotes, where in many cases the recommendation does not differ from that given in JPL10-6. Further details of the present evaluation are given below.

No experimental data are available for the 10 fully halogenated compounds. For CCl_3F, CCl_2F_2, CCl_4, $CBrClF_2$, $CBrF_3$, CBr_2F_2, and $CBrF_2CBrF_2$ the recommended kinetic parameters were estimated by setting the Arrhenius pre-exponential factor (A) to 1×10^{-10} cm^3 $molecule^{-1}$ s^{-1} and the activation energy (E) to the reaction endothermicity using available thermochemical parameters (Atkinson *et al.*, 2008; Sander *et al.*, 2011). This procedure results in upper limits for the reaction-rate coefficients that are considerably less than those reported in laboratory studies that are often limited by the capabilities of the experimental techniques. For CCl_2FCClF_2 (CFC-113), $CClF_2CClF_2$ (CFC-114), and CF_3CClF_2 (CFC-115), where thermochemical data for reaction products are not available, the recommended activation energy for CCl_4 was assigned. The estimated activation energy for CCl_4 is the lowest among the fully halogenated compounds not containing Br that have known reaction product thermochemistry. The rate coefficients for the three fully halogenated chlorofluoroethanes are expected to be less than that for CCl_4 because the presence of fluorine increases the reaction endothermicity; see the trend in endothermicity for the fluorinated molecules given in Table 3.1.

The recommended pre-exponential factors and the activation energies are unchanged from the JPL10-6 recommendations for CHF_2Cl (HCFC-22), N_2O, CH_4, CHF_3 (HFC-23), CH_3Br, and CHF_2CF_3 (HFC-125). Minor changes to the JPL10-6 recommendations were made for CH_3CCl_3, CH_3CFCl_2 (HCFC-141b), CH_3CClF_2 (HCFC-142b), CH_3Cl, and CH_3CHF_2 (HFC-152a) based on slight differences in the way that the multiple data sets were combined for analysis (see Table 3.3 footnotes). For CH_2F_2 (HFC-32) the difference in the recommended parameters stems from the inclusion of a recent laboratory study that was conducted after the JPL10-6 evaluation was finalized. For CH_2FCF_3 (HFC-134a) and CF_3CH_3 (HFC-143a) the differences from the JPL10-6 recommendations are more significant. For CH_2FCF_3 (HFC-134a) the difference is due to the consideration of a recent study (Nilsson *et al.*, 2009) made after JPL10-6 was finalized and by only considering experimental data at temperatures <330 K because of slight non-Arrhenius behavior (curvature). For CF_3CH_3 (HFC-143a), the JPL10-6 recommendation is revised following the consideration of the room-temperature rate coefficient reported by Nielsen *et al.* (1994) (see Table 3.3 footnote and supplement). The reactions for CF_3CHFCF_3 (HFC-227ea) and $CHF_2CH_2CF_3$ (HFC-245fa) were not included in the JPL10-6 evaluation. Only 298 K experimental data are available for these reactions and E/R was estimated by comparison with compounds having similar halogen substitution and similar reactivity at 298 K.

3.3 Photochemical Loss Processes

The evaluation of the Vacuum Ultraviolet (VUV) and Ultraviolet (UV) absorption spectra presented here was based on an examination of published experimental data. It includes recommendations for hydrogen Lyman-α (121.567 nm) absorption cross sections, σ(L-α), as well as absorption spectra and their temperature dependences for wavelengths (λ) >169 nm. As part of this evaluation, a critical assessment of the wavelength and temperature-dependent uncertainties in the recommended cross sections was made in order to better quantify uncertainties in atmospheric photolysis lifetime calculations. A brief summary of the evaluation is given below.

Currently there are no UV (λ >169 nm) absorption spectrum data available for the hydrofluorocarbons (HFCs) CH_2FCF_3 (HFC-134a), CH_3CF_3 (HFC-143a), CHF_3 (HFC-23), CH_2F_2 (HFC-32), CHF_2CF_3 (HFC-125), CH_3CHF_2 (HFC-152a), CF_3CHFCF_3 (HFC-227ea), and $CHF_2CH_2CF_3$ (HFC-245fa) or for CH_4 (methane) due primarily to their weak absorption in this wavelength region. The UV absorption cross sections for these compounds at λ >169 nm are expected to be sufficiently small that atmospheric photolysis in this wavelength region would make a negligible contribution to that molecule's atmospheric loss and, therefore, are not considered further.

Table 3.4 gives the σ(L-α) values for each of the molecules included in this report. The JPL10-6 evaluation provided a σ(L-α) recommendation for N_2O and citations to the literature for several other molecules. The recommended σ(L-α) values and uncertainty estimates given in Table 3.4 were derived from an evaluation of the available experimental data, all of which were obtained at room temperature, nominally 298 K. In cases where no experimental data are available, σ(L-α) values were estimated based on the measured cross sections for similar molecules. For the HFCs and HCFCs, σ(L-α) exhibits a trend of decreasing cross sections with increasing F atom substitution that was used to estimate cross-section values in some cases.

For the majority of the compounds included in this report for which UV (λ >169 nm) absorption spectra are available, the cross-section recommendations and their temperature dependences are as recommended in JPL10-6. The exceptions are CCl_4, CF_2Br_2 (Halon-1202), CF_2ClBr (Halon-1211), and CF_2BrCF_2Br (Halon-2402) where new laboratory measurements have become available since the JPL10-6 recommendations were finalized and CF_3Br (Halon-1301), CH_3CClF_2 (HCFC-142b), and NF_3 where specific recommendations were not provided in JPL10-6. In addition, inaccuracies in the cross-section parameterizations for $CFCl_3$ (CFC-11), CF_2Cl_2 (CFC-12), $CFCl_2CF_2Cl$ (CFC-113), CF_2ClCF_2Cl (CFC-114), CH_3CCl_3, CH_3Cl, and CHF_2Cl (HCFC-22) given in the literature and quoted in JPL10-6 from the original publications (Simon *et al.,* 1988a, b) are corrected here (see supplementary material).

Recommended uncertainties in the absorption cross sections, as well as in their temperature dependences, are given in Table 3.4. The estimated uncertainties are not statistical quantities, but rather are based on an evaluation of the reliability of the experimental measurements and the level of agreement among different studies where available. The uncertainties in an absorption spectrum and in its absolute cross sections are generally wavelength dependent, where the weaker absorption regions of a spectrum usually have greater uncertainty. Uncertainty parameters are provided for σ(L-α) and for the wavelength ranges 169-190, 190-230, 230-286, and >286 nm in order to provide an analysis that is sufficiently detailed to permit evaluation of the wavelength regions that are most critical to the photolytic loss of these molecules. For example, HFCs do not undergo UV photolysis and are photolyzed in the atmosphere primarily by absorption at Lyman-α, while Halons are lost by a combination of UV photolysis in the 190-230 and >286 nm regions where the relative importance of these wavelength regions is altitude dependent and quantified using an atmospheric model as shown later in this chapter.

The cross-section uncertainties given here are parameterized using a formalism similar to that used for gas-phase reaction-rate coefficients where p(298 K) represents the 2σ (95% confidence) level uncertainty in the 298 K absorption cross-section data and w is a parameter used to represent the increase in the cross-section 2σ uncertainty at other temperatures

$$p(\mathrm{T}) = p(298\ \mathrm{K})\ exp\left(\left|w\left(\frac{1}{\mathrm{T}} - \frac{1}{298}\right)\right|\right)$$

The JPL10-6 evaluation provides estimated uncertainties for the product of the absorption cross sections and photolysis quantum yields for N_2O, CCl_4, $CFCl_3$, CF_2Cl_2, CF_3Br, CF_2ClBr, and CF_2BrCF_2Br. The uncertainty estimates provided in this chapter were derived for the absorption cross sections alone, but can be compared with those reported in JPL10-6 assuming a quantum yield of unity for photolytic loss of the compound.

As indicated above, there are a number of compounds for which the UV cross-section recommendations in this assessment differ from those given in JPL10-6. Details of these differences are as follows.

CCl_4 (Carbon Tetrachloride): A recent study by Rontu *et al.* (2010) reported CCl_4 absorption cross sections at 183.95, 202.206, 206.200, 213.857, and 228.8 nm, using atomic line sources, and the spectrum between 200 and 235 nm measured using diode array spectroscopy. Their results are in agreement with previously reported values that are discussed in JPL10-6, but are of higher precision and accuracy. The uncertainty factor given in Table 3.4 is reduced from that given in JPL10-6 primarily due to inclusion of these new results. For the temperature dependence of the cross sections, JPL10-6 recommends the parameterization reported by Simon *et al.* (1988b) (174-250 nm; 225-295 K), which reproduces their experimental values to within ±5%. The revised CCl_4 absorption cross-section parameterization reported in Rontu *et al.* (given below) is recommended here, while the uncertainty parameters given in Table 3.4 encompass the range of the data from the Rontu *et al.* and Simon *et al.* studies.

Absorption cross-section parameterization for CCl_4 taken from Rontu *et al.* (2010)

$$\log_{10}\sigma(\lambda,\mathrm{T}) = \sum_i A_i\lambda^i + (\mathrm{T} - 273)\sum_i B_i\lambda^i$$

CCl_4 (Carbon Tetrachloride)		
i	A_i	B_i
0	1112.736208	-1.116511649
1	-22.02146808	0.02447268904
2	0.1596666745	-0.0001954842393
3	-0.0005104078676	$6.775547148 \times 10^{-7}$
4	$6.062440506 \times 10^{-7}$	$-8.621070147 \times 10^{-10}$

CF_2ClBr (Halon-1211): The recommendations provided here are based on the studies reviewed in JPL10-6 together with the recent investigation by Papanastasiou *et al.* (2013) who reported CF_2ClBr absorption cross sections between 300 and 350 nm that included corrections for Rayleigh scattering. The room temperature cross sections recommended here are a combination of the JPL10-6 recommendation for $\lambda < 260$ nm and the parameterization reported in Papanastasiou *et al.* for $\lambda \geq 260$ nm. The recommendation for the cross-section temperature dependence in the short-wavelength region is taken from Burkholder *et al.* (1991) (190-320 nm; 210-296 K). In the long-wavelength region, $\lambda \geq 260$ nm, the cross-section parameterization recommendation (given below) is taken from Papanastasiou *et al.*, which was derived from their data and the data of Gillotay and Simon (1989) (169-302 nm; 210-295 K) and Burkholder *et al.* (1991) (190-320 nm; 210-296 K). The uncertainty factors

given in Table 3.4 are significantly reduced from those reported in JPL10-6 due primarily to the consideration of the Papanastasiou *et al.* study.

CF_3Br (Halon-1301): The recommendation given here for the room temperature absorption spectrum is the same as JPL10-6. There are currently no available Halon-1301 cross-section data for wavelengths >300 nm, however, this region makes only a minor contribution to the calculated photolytic lifetime as shown in Section 3.5. No recommendation was given in JPL10-6 for the spectrum temperature dependence, although the cross-section parameterizations reported in Gillotay and Simon (1989) (178-280 nm, 210-300 K) and Burkholder *et al.* (1991) (190-285 nm, 210-296 K) were provided. The cross-section temperature dependences in the short-wavelength region from these studies are in relatively poor agreement, e.g., differences of ~20% at 205 nm and 210 K. Differences in the absolute cross-section values and their temperature dependence in the longer-wavelength region, λ >260 nm, exist between the data sets as well, e.g., the difference at 270 nm and 250 K is ~30%. The parameterization from Burkholder *et al.* (1991) is recommended here. The uncertainty factors given in Table 3.4 cover the range of the reported values in the various wavelength regions.

CH_3CF_2Cl (HCFC-142b): The recommendations given here for the CH_3CF_2Cl absorption cross sections and their temperature dependence are from the parameterization given by Nayak *et al.* (1996). JPL10-6 does not make a recommendation for the cross-section temperature dependence, but does report the parameterizations from Gillotay and Simon (1991), Orlando *et al.* (1991), and Nayak *et al.* The results from Nayak *et al.* and Gillotay and Simon differ significantly at shorter wavelengths, but are in reasonable agreement in the critical wavelength region for atmospheric photolysis, 205-220 nm, while the data from Orlando *et al.* and Hubrich and Stuhl (1980) are systematically different. The uncertainty factors given in Table 3.4 reflect the level of agreement between the Nayak *et al.* and the Gillotay and Simon studies.

CF_2Br_2 (Halon-1202): The recommendations provided here for the CF_2Br_2 cross sections and their temperature dependence in the $\lambda \geq 260$ nm region (given below) are based on the analysis provided by Papanastasiou *et al.* (2013) who reported absorption cross-section data in the long-wavelength region (300-325 nm; 210-296 K) that were corrected for Rayleigh scattering. For $\lambda < 260$ nm, the cross-section parameterization given in Burkholder *et al.* (1991) is recommended here. The uncertainty factors given in Table 3.4 are significantly lower than reported in JPL10-6 and encompass the range of the majority of the available experimental data.

CF_2BrCF_2Br (Halon-2402): The recommendations provided here for the CF_2BrCF_2Br cross sections and their temperature dependence are based on the studies reviewed in JPL10-6 together with the recent investigation and analysis by Papanastasiou *et al.* (2013) who reported absorption cross-section data in the long-wavelength region (300-325 nm; 250, 270, and 296 K) that were corrected for Rayleigh scattering. The 298 K cross sections recommended here are taken from JPL10-6 for $\lambda < 260$ nm and from Papanastasiou *et al.* for $\lambda \geq 260$ nm. For the temperature dependence at $\lambda < 260$ nm the parameterization of Gillotay *et al.* is recommended here. In the long-wavelength region, the cross-section parameterization reported in Papanastasiou *et al.* (given below) is recommended. The uncertainty factors given in Table 3.4 are significantly lower than reported in JPL10-6 and cover the range of the available experimental data, except in the long-wavelength region where the superseded data from Burkholder *et al.* (1991) fall outside the given range.

Absorption cross-section parameterizations for CF_2ClBr (Halon-1211), CF_2Br_2 (Halon-1202), and CF_2BrCF_2Br (Halon-2402) for wavelengths ≥260 nm and temperatures between 210 and 298 K as taken from Papanastasiou *et al.* (2013)

$$\ln\left(\sigma(\lambda,T)\right) = \sum_i A_i\left(\lambda - \bar{\lambda}\right)^i \times \left[1 + (296 - T)\sum_i B_i\left(\lambda - \bar{\lambda}\right)^i\right]$$

CF_2ClBr (Halon-1211)		
$\bar{\lambda}$ = 280.376		
i	A_i	B_i
0	-48.3578	0.0002989
1	-0.1547325	8.5306×10^{-6}
2	-4.966942×10^{-4}	4.26×10^{-8}
3	1.56338×10^{-6}	-1.84×10^{-9}
4	3.664034×10^{-8}	1.284×10^{-11}
CF_2Br_2 (Halon-1202)		
$\bar{\lambda}$ = 287.861		
i	A_i	B_i
0	-47.4178	0.0003173
1	-0.1567273	1.2323×10^{-5}
2	-2.624376×10^{-4}	2.68×10^{-8}
3	-6.78412×10^{-6}	-5.28×10^{-9}
4	1.261478×10^{-7}	6.99×10^{-11}
CF_2BrCF_2Br (Halon-2402)		
$\bar{\lambda}$ = 274.64		
i	A_i	B_i
0	-48.3611	0.0001877
1	-0.1595	7.252×10^{-6}
2	-1.026×10^{-4}	2.917×10^{-7}
3	-1.334×10^{-5}	-1.725×10^{-9}
4	1.458×10^{-7}	-2.675×10^{-11}

NF_3 (Nitrogen trifluoride): JPL10-6 did not include an evaluation of the NF_3 UV absorption spectrum. The room temperature UV absorption spectrum has been reported by Makeev *et al.* (1975), Molina *et al.* (1995) (180-250 nm), Dillon *et al.* (2010) (184-226 nm), and Papadimitriou *et al.* (2013) (185-250 nm), where the wavelength range of the reported spectrum is given in parentheses. The spectrum reported by Makeev *et al.* seems to be in error and was not considered further. The agreement between the Molina *et al.*, Dillon *et al.*, and Papadimitriou *et al.* studies is good, to within ~5%, over the wavelength range most critical for atmospheric photolysis, 200 to 220 nm. Papadimitriou *et al.* also reported absorption cross-section data at 212, 231, 253, 273, and 296 K. The wavelength and temperature-dependence parameterization reported by Papadimitriou *et al.*, see table below, is recommended here.

Absorption cross-section parameterization for NF_3 valid between 184.95 and 250 nm and the temperature range 212 to 296 K

$$\log_{10}\sigma(\lambda,T) = \sum_i A_i\lambda^i + (296 - T)\sum_i B_i\lambda^i$$

NF_3 (Nitrogen trifluoride)		
i	A_i	B_i
0	-218.67	0.9261
1	4.03743	-0.0130187
2	-0.0295605	6.096×10^{-5}
3	9.596×10^{-5}	-9.75×10^{-8}
4	-1.3171×10^{-7}	9.76×10^{-12}
5	4.929×10^{-11}	–

3.4 Other Processes

Atmospheric heterogeneous loss processes involve chemical and physical interactions of gases with liquid and solid phases, i.e., clouds and aerosols. The composition of the condensed phases found in the atmosphere are multi-component where aqueous droplets, for example, may contain inorganic salts, sulfuric acid, and semi-volatile organics, while solid particles may consist of ice, soot, or mineral dust. Consequently, heterogeneous loss processes depend on the nature of the condensed phase, temperature, relative humidity, reactivity, and mass transport. For the majority of the molecules included in this report heterogeneous loss processes are expected to be minor, but are not well defined. Henry's Law (solubility) coefficients are evaluated in JPL10-6 and Staudinger and Roberts (2001) for a number of molecules considered in this report. Henry's Law coefficients used in Chapter 4 were not evaluated in this chapter.

Lu and Sanche (2001) and Lu (2009; 2010) have proposed that cosmic-ray induced heterogeneous chemistry may contribute to stratospheric loss of chlorofluorocarbons (CFCs). The proposed mechanism would, therefore, contribute to ozone depletion, particularly in the polar regions. The significance of this mechanism on stratospheric chemistry has been debated in the literature (Harris *et al.*, 2002; Müller, 2003; Patra and Santhanam, 2002). It has been shown that both observed stratospheric CFC distributions and tracer-tracer correlations of CFCs with long-lived species are not compatible with a significant destruction of CFCs on polar stratospheric clouds (PSC) (Grooß and Müller, 2011; Müller, 2003; Müller and Grooß, 2009). Thus, cosmic-ray induced heterogeneous reactions are not considered a significant stratospheric loss process for CFCs and not an alternative mechanism causing the Antarctic ozone hole (Grooß and Müller, 2011; Müller, 2003; Müller and Grooß, 2009).

3.5 Lifetimes, Uncertainties, and Ranges

The NASA/Goddard Space Flight Center (GSFC) two-dimensional (2-D) coupled chemistry-radiation-dynamics model was used to evaluate the impact of the kinetic and photochemical recommendations on atmospheric lifetimes. Model calculations were performed using input from the recommendations given in this report as well as those from JPL10-6 for comparison purposes. The GSFC 2-D model has been used in stratospheric ozone assessments (WMO, 2007; 2011), and in studies pertaining to the chemistry-climate coupling of the middle atmosphere. The residual circulation framework used in 2-D models has been shown to provide realistic simulations of atmospheric transport on long timescales (>30 days). As

demonstrated in recent studies, the model ozone, temperature, zonal wind, and long-lived tracer simulations are in good overall agreement with a variety of observations in reproducing transport-sensitive features in the meridional plane (Fleming *et al.*, 2011). The computational speed of the 2-D model allowed numerous sensitivity simulations to be performed as part of this evaluation as outlined in Table 3.5. The GSFC 2-D model is, therefore, a useful tool to evaluate the atmospheric lifetimes for the molecules included in this report, as well as the relative importance of the different atmospheric loss processes and the lifetime sensitivity to the recommended kinetic and photochemical parameters and their uncertainties. The GSFC 2-D model was also used in Chapter 5, "Model Estimates of Lifetimes", allowing for traceability between the 2-D and 3-D model calculated lifetimes.

The 2-D model calculations were used to (1) calculate local and global annually averaged lifetimes, (2) quantify the relative contributions of the reactive and photolytic loss processes to the local and global lifetimes, (3) compare lifetimes obtained using the SPARC and JPL10-6 recommended model input parameters, (4) evaluate the impact of Lyman-α photolysis (not included in JPL10-6) on calculated lifetimes, (5) quantify the range in calculated atmospheric lifetimes due to the uncertainties in the model input kinetic and photochemical parameters, and (6) evaluate the lifetime sensitivity to uncertainties in the O_2 and O_3 absorption cross sections.

The 2-D model results presented in this chapter are from steady-state simulations for year 2000 conditions of source gas loading, solar flux, and stratospheric aerosol density. These conditions are consistent with the year 2000 time slice model simulations and analysis presented in Chapter 5. The model tropospheric OH was specified from the monthly-varying OH field documented in Spivakovsky *et al.* (2000) following the methodology used in Chapter 5. Reaction with the OH radical is an important atmospheric removal process for many of the molecules included in this assessment, i.e., the hydrogen containing molecule lifetimes are largely determined by the rates of their OH reactions. Since the majority of the OH reactive loss occurs in the troposphere, specifying the tropospheric OH field in this manner was important for analysis of model simulations of the OH related loss rates and lifetimes. The lifetime sensitivity to the OH field is discussed further in Chapter 5. The stratospheric and mesospheric OH, and atmospheric $O(^1D)$ and Cl atom profiles are simulated by the model for all calculations presented in this chapter. Global annual averages are given here, consistent with the general methodology used to compute the lifetimes (Kaye *et al.*, 1994). Lifetimes are computed as the ratio of the global atmospheric burden to the vertically integrated annually averaged global total loss rate (Kaye *et al.*, 1994), consistent with the methodology used in the model simulations for Chapter 5.

Model results for CHF_2Cl, HCFC-22, obtained using the SPARC recommendations are given graphically here for example purposes, while a complete set of results for all the molecules is presented in the tables and graphical supplementary material. The calculated local lifetimes for the various loss processes as well as the total local lifetime are shown in Figure 3.3. The figure includes all of the loss processes, although not all make a significant contribution to the total local lifetime. To identify the wavelength regions of greatest importance in the photolytic loss, the photolytic loss was divided into Lyman-α and the wavelength ranges 169-190, 190-230, 230-286, and >286 nm. For HCFC-22, atmospheric loss in the troposphere is dominated by its reaction with the OH radical. In the middle to upper stratosphere reaction with $O(^1D)$ contributes to its loss with photolysis in the 190-230 nm wavelength region making a minor contribution. In the mesosphere above 65 km, HCFC-22 loss is dominated by Lyman-α photolysis.

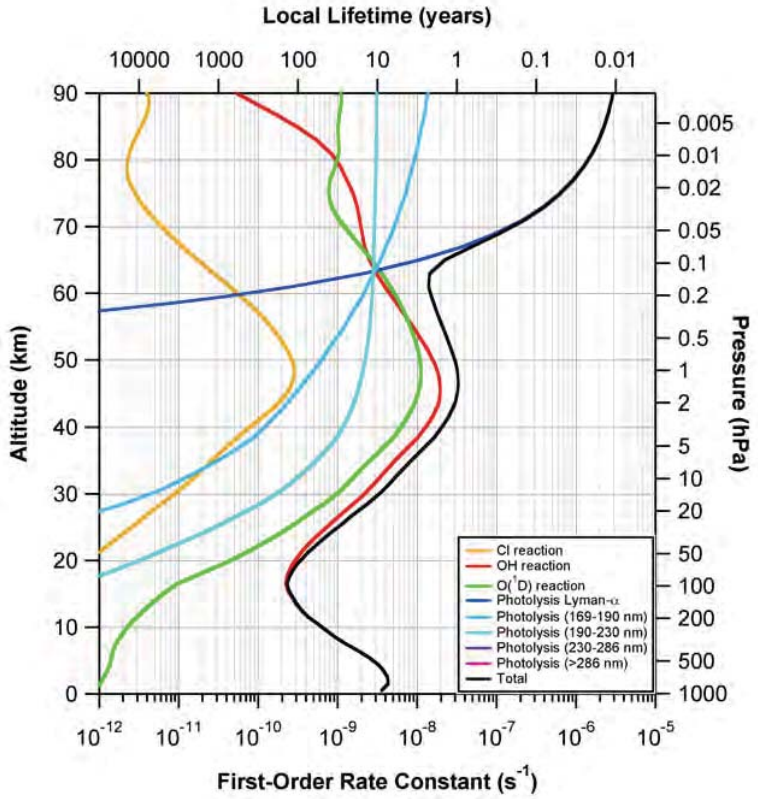

Figure 3.3. Global annually averaged local lifetimes for various gas-phase loss processes of CHF_2Cl (HCFC-22) calculated using the GSFC 2-D model for year 2000 steady state conditions.

The calculated atmospheric molecular loss rate and mixing ratio vertical profiles for HCFC-22 are shown in Figure 3.4. The molecular loss rate is greatest at Z = 0 and decreases significantly throughout the troposphere. The global annually averaged lifetime for HCFC-22 was calculated to be 12.2 years, while the lifetime obtained using the JPL10-6 parameters is slightly less, 12.0 years. The global lifetimes for each compound calculated using the SPARC and JPL10-6 recommended model input parameters are given in Tables 3.6 and 3.7. The differences in lifetimes obtained using the JPL10-6 and present recommended parameters are generally small, <5%, for most of the molecules. However, for CCl_4, the difference is substantial, 38.0 (JPL10-6) vs. 48.7 (SPARC) years, owing to the greater OH reactive loss obtained using the JPL10-6-recommended rate-coefficient upper limit for the OH + CCl_4 reaction. The rate-coefficient upper limit is significantly reduced in the present SPARC recommendation and, thus, represents a negligible loss process and in turn yields a longer and more representative lifetime. The lifetime difference is also large for Halon-2402, 13.9 (JPL10-6) vs. 27.8 (SPARC) years, due to the greater photolytic loss at wavelengths >286 nm obtained using the JPL10-6 recommendation and for CFC-115 (961 (JPL10-6) vs. 540 (SPARC) years) due to the change in its $O(^1D)$ rate coefficient. The lifetime differences for Halon-1211, Halon-1202, and HFC-227ea are less and on the order of ~20%.

Table 3.6 also gives the fractional contributions to the calculated lifetime from the photolytic and $O(^1D)$, OH, and Cl reactive losses for each molecule. The fractional contribution breakdown identifies the most critical loss processes for each molecule as well as potential focus areas for future laboratory studies. The fractional contributions obtained using the

present and JPL10-6 recommendations are also given graphically in Figure 3.5. The figure illustrates that photolysis is the dominant loss process for most of the species primarily removed in the stratosphere (including the Halons), while reaction with OH is the dominant atmospheric loss process for the hydrogen containing compounds. For example, for HCFC-22, OH reactive loss accounts for 98.2% of its global annually averaged loss, while $O(^1D)$ reaction contributes 1.4% and photolysis 0.4%.

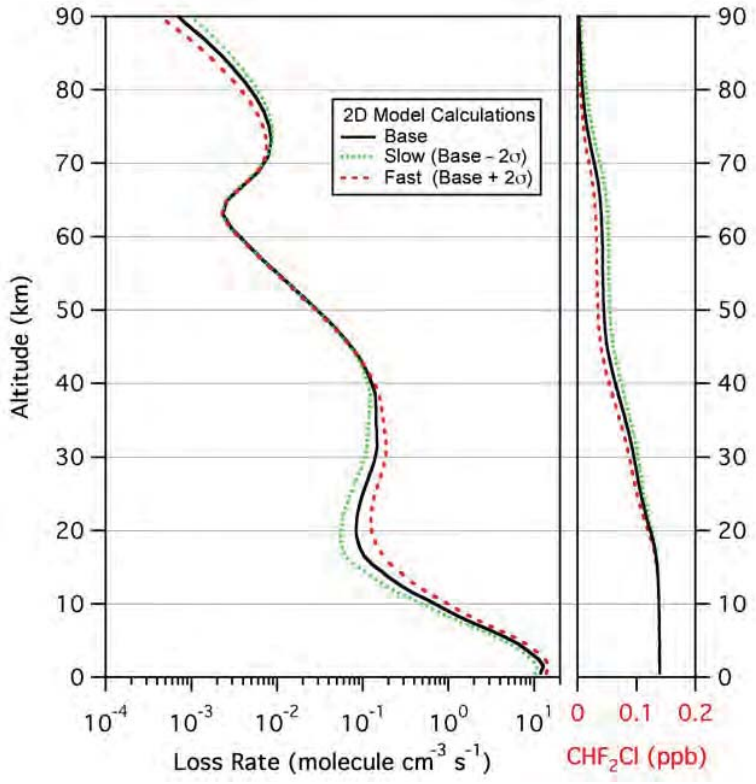

Figure 3.4. Global annually averaged vertical profile molecular loss rates and mixing ratios for CHF_2Cl (HCFC-22) calculated using the GSFC 2-D model and SPARC kinetic and photochemical parameter recommendations for year 2000 steady state conditions.

In summary, the key 2-D model global annually averaged findings include:

- For the hydrogen containing compounds, reaction with the OH radical is the dominant atmospheric removal process (>90% of the total loss) and occurs primarily in the troposphere for most of the molecules in this study.
- For N_2O (nitrous oxide), NF_3, the CFCs, and CCl_4, photolysis is a dominant loss process (37% for CFC-115, 70-75% for NF_3 and CFC-114, and >90% for the others,) with stratospheric photolysis in the 190-230 nm region accounting for >90% of the photolytic loss (75% of the photolytic loss for CFC-115).
- For the Halons, photolysis is the dominant loss process (>97%) with altitude dependent contributions from both the 190-230 and >286 nm wavelength regions.
- The $O(^1D)$ reactive loss is significant for CFC-114 (25%), CFC-115 (63%), N_2O (10%), and NF_3 (28.7%) but <6% for other molecules considered in this study.

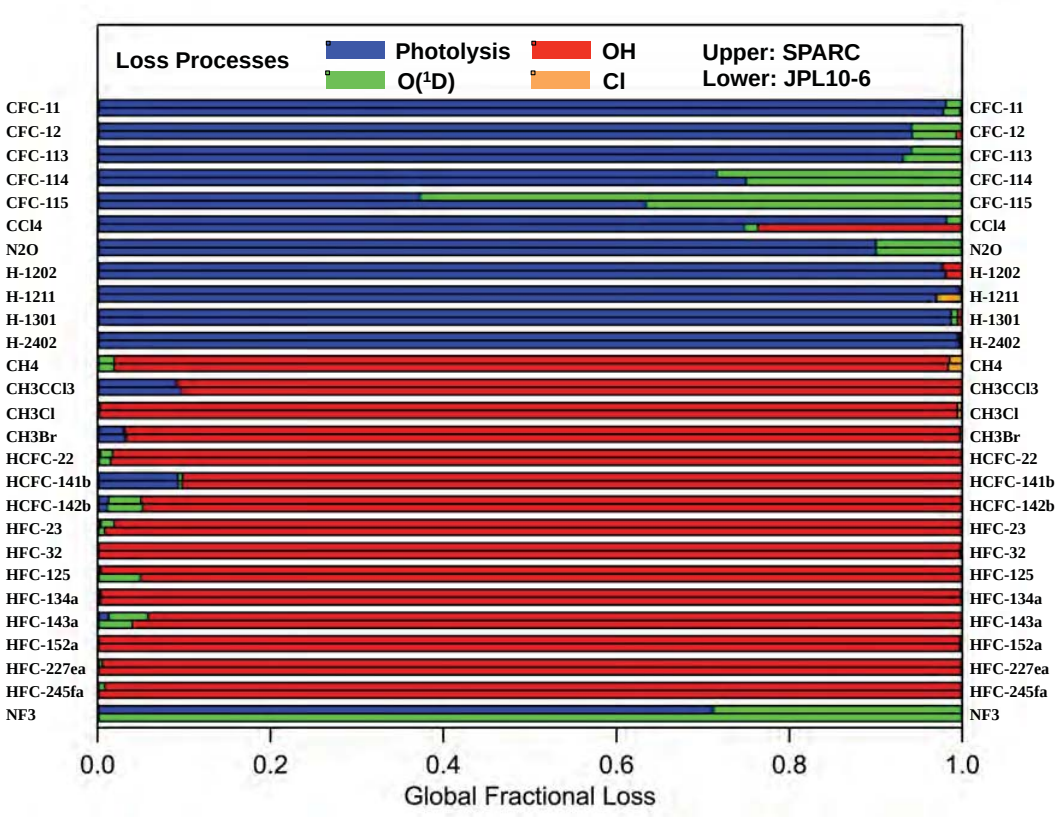

Figure 3.5. Summary of the global annually averaged fractional losses (see legend) obtained using the 2-D model with kinetic and photochemical input parameters from SPARC (upper bar) and JPL10-6 (lower bar).

- Overall, atmospheric loss due to Cl atom reaction is minor, <1.5% for CH_4 and <0.5% for all other molecules in this study.

An objective of this chapter was to evaluate the uncertainty (range) in calculated atmospheric lifetimes due to the uncertainties in the model input kinetic and photolytic parameters given in Tables 3.1 – 3.4. To do this, model simulations were made with the input parameters set to their 2-σ uncertainty lowest values (slow) and to their 2-σ uncertainty greatest values (fast) and compared with the baseline calculations presented above. However, a complication is that changes to the model input parameters impact all model calculated trace species including ozone. Changes in ozone modify the incident solar radiation in the atmosphere, which impacts the calculated lifetimes via changes in the photolysis of trace species, production of $O(^1D)$, and the concentration of stratospheric OH. To aid an evaluation of this feedback, two sets of model simulations were each made for the slow and fast scenarios: 1) all model constituents including ozone allowed to interact in standard fashion, and 2) as in 1), except with the molecules addressed in this report treated as non-interactive tracers so that changes to their kinetic and photolytic parameters will not impact ozone. Table 3.5 summarizes the model simulations performed.

The annually averaged ozone impacts of the slow and fast interactive simulations, using the SPARC model parameters, are shown in the top panels of Figure 3.6. The ozone change from the baseline calculation is generally small, <5%, but not negligible. In the slow case,

the change in ozone increases in the middle-upper stratosphere, but decreases in the troposphere and tropical lower stratosphere. For the fast case, the ozone changes from baseline are roughly equal and opposite to those in the slow case. The ozone changes in the mesosphere, above 60 kilometers (km), are generally small, <1%, and are not shown in Figure 3.6.

The vast majority of the ozone change in the slow/fast calculations is due to the changes in the kinetic parameters for the reactions of CH_4 with OH, $O(^1D)$, and Cl and the photolysis of N_2O and its reaction with $O(^1D)$. Changes in the kinetic and photolytic parameters of the other molecules included in this study have a minimal impact on ozone. Changes in the CH_4 reactions impact ozone via the inorganic chlorine (Cl_x) and odd hydrogen (HO_x) ozone-loss cycles in the stratosphere and the NO_x-induced ozone production cycle in the troposphere and lower stratosphere. The change in ozone due to the changes in the three CH_4 loss processes is shown in the middle panels in Figures 3.6. The net impact in the slow (fast) case yields ozone increases (decreases) of 1% in the upper stratosphere, ozone decreases (increases) of 1-2% in the upper troposphere-lower stratosphere, and ozone decreases (increases) of 6-7% in the ozone hole region.

Changes in the N_2O loss parameters impact stratospheric ozone via direct changes in the abundance of odd-oxygen ($O + O_3$) due to N_2O photolysis, and odd-nitrogen ($NO + NO_2$) due to the N_2O reaction with $O(^1D)$. The net impact on ozone is shown in the bottom panels in Figure 3.6. The net impact of the slow (fast) N_2O loss yields increases (decreases) in ozone of 4-5% in the global middle-upper stratosphere and polar lower stratosphere. Smaller ozone changes occur at lower altitudes that are likely caused by a "shielding" effect. In general, ozone increases at lower altitudes due to ozone depletion above are known in the literature as "self-healing" events and have been discussed previously (Harrison, 1975).

For almost all molecules, including the ozone feedback yielded a somewhat larger range of lifetimes between the slow and fast calculations. Exceptions to this are CFC-114 and CFC-115 that have weak tropospheric losses and large mesospheric losses. The ozone feedback had the largest impact on CFC-115, with lifetime differences of ~10% between the interactive and non-interactive cases. For compounds that have significant or dominant stratospheric losses (CFC-11, CFC-12, CFC-113, CFC-114, CCl_4, N_2O, and Halon-1301), the feedback effect is minor, with lifetime differences in the range 1.5 to 4%. For compounds that have a dominant tropospheric OH loss, the ozone feedback effect is small since tropospheric OH is specified in the model. For these compounds, the lifetime differences are <0.6% between the interactive and non-interactive cases.

Using the model calculations with the ozone feedback included, the uncertainty in the local lifetime was calculated from the slow and fast case results. Figure 3.7 shows the uncertainty in the local loss rate for HCFC-22 and a breakdown of the contribution from the different loss processes. The uncertainty at Z = 0 is ~18% due almost exclusively to the uncertainty in the OH + HCFC-22 reaction-rate coefficient. The increase in the uncertainty with increasing altitude throughout the troposphere and lower stratosphere is due to the increased uncertainty in the rate coefficient at lower temperatures.

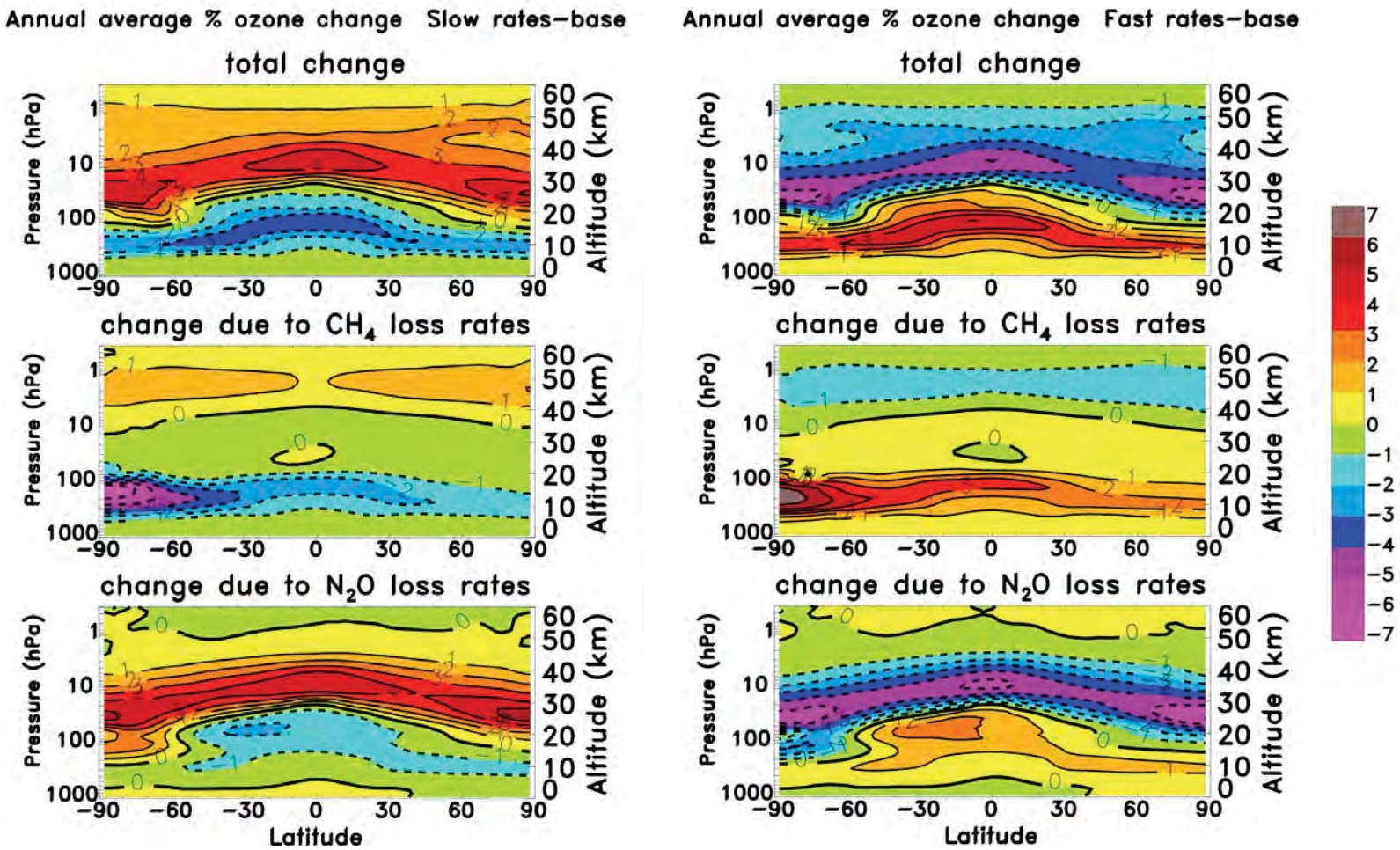

Figure 3.6. Annually averaged percentage ozone change in the slow and fast (see text) model simulations (top) for all 26 compounds, (middle) CH_4 only; (bottom) N_2O only. The ozone change is taken relative to the Baseline case using steady-state model simulations for year 2000 conditions as discussed in the text**.** The contour interval is ±1%.

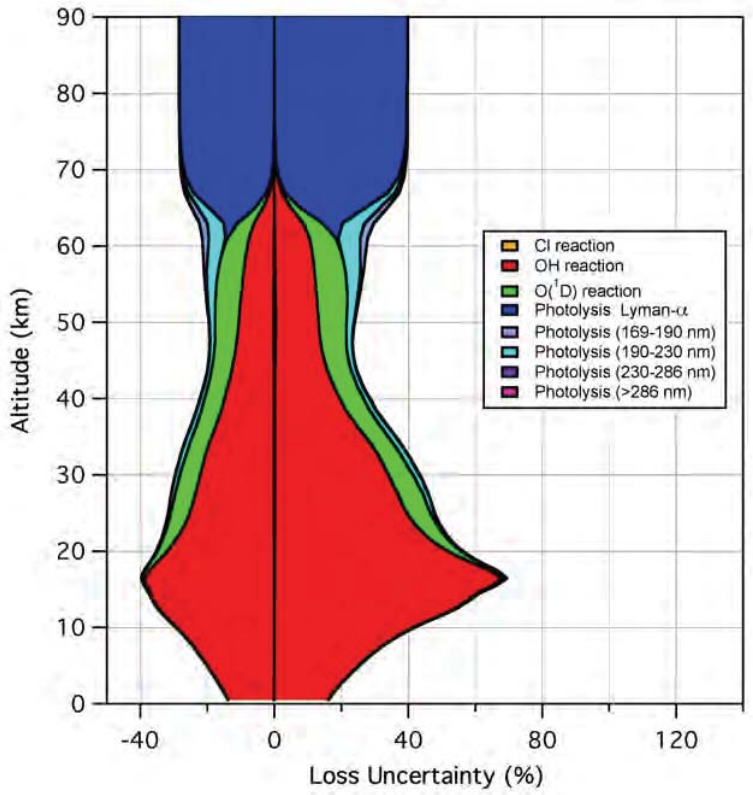

Figure 3.7. Uncertainty in the global annually average local loss rate from the GSFC 2-D model calculation with the SPARC recommended parameters and uncertainties for CHF_2Cl (HCFC-22).

The range in the HCFC-22 global lifetime computed from the fast (minimum lifetime) and slow (maximum lifetime) uncertainty limits with the ozone feedback included is 10.0 to 14.9 years, a ~±20% difference from the baseline lifetime value. The vertical molecular loss and mixing ratio profiles for the slow and fast cases are included in Figure 3.4 for comparison with the baseline calculation. The range in global lifetimes for all the molecules is given in Table 3.7. There is a wide variation in the lifetime ranges among the molecules; the percentage range is smallest, ~5-10%, for N_2O, CCl_4, and the CFCs (excluding CFC-115).

The 2-D model calculated lifetimes obtained using the SPARC and JPL10-6 input kinetic and photochemical parameters are also given graphically in Figure 3.8, where the whiskers represent the 2σ range in the calculated lifetime due solely to the estimated uncertainty in the input parameters.

Table 3.7 also gives the lifetimes separated by the troposphere (surface to the tropopause, seasonally and latitude-dependent), stratosphere, and mesosphere (<1 hPa). The lifetimes are computed using the global atmospheric burden and the loss rate integrated over the different atmospheric regions such that

$$\frac{1}{\tau_{\text{Tot}}} = \frac{1}{\tau_{\text{Trop}}} + \frac{1}{\tau_{\text{Strat}}} + \frac{1}{\tau_{\text{Meso}}}$$

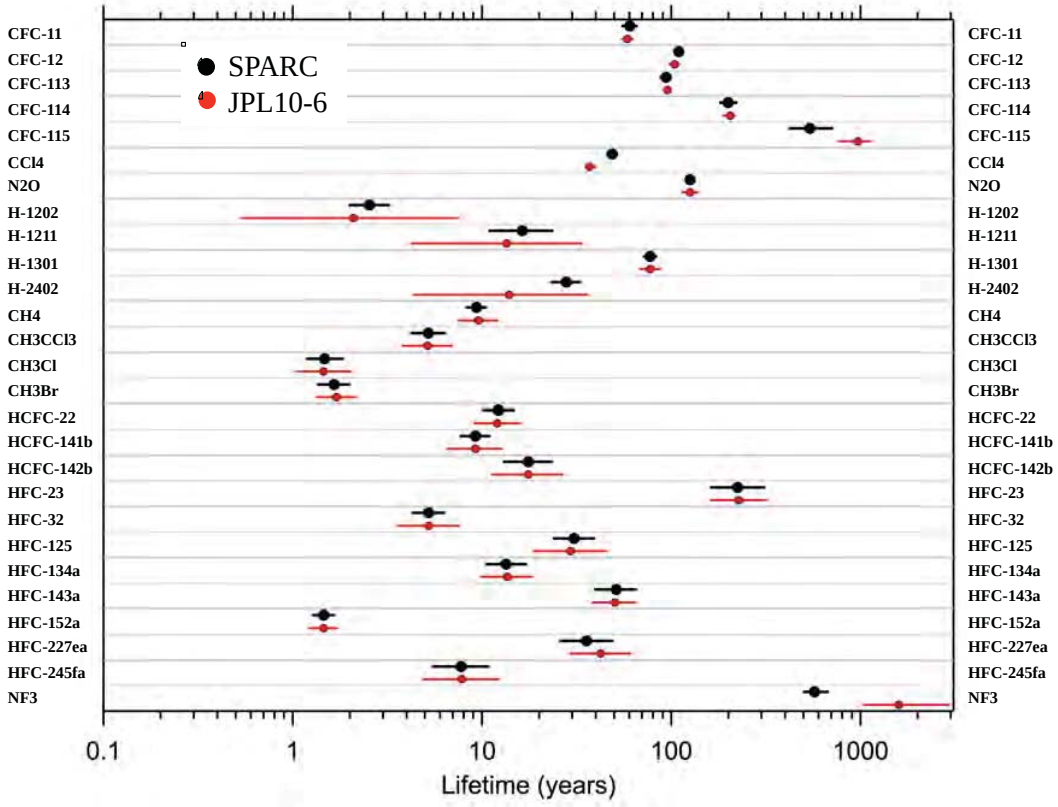

Figure 3.8. Summary of the global annually averaged lifetimes obtained using the 2-D model with kinetic and photochemical input parameters from SPARC (black, upper) and JPL10-6 (red, lower) values reported in Tables 3.6 and 3.7. The whisker error bars show the 2σ range in the calculated lifetime due solely to the uncertainty in the kinetic and photochemical input parameters.

Molecules with short tropospheric lifetimes reflect a dominant OH reactive loss, or for Halon-1211 and Halon-1202, a dominant photolysis loss at wavelengths >286 nm. Most molecules have very long mesospheric lifetimes (>10,000 years); CFC-114, CFC-115, HCFC-22, HCFC-142b, CH_4, and some of the HFCs have mesospheric lifetimes between 2,500 and 4,900 and years.

3.6 Lifetime Sensitivity to O_2 and O_3 UV Cross Sections

O_2 and O_3 absorption cross sections used in models are important in quantifying the amount of UV radiation incident at any point in the atmosphere, and in determining the concentration of ozone throughout the middle atmosphere. Uncertainties in the O_2 and O_3 cross sections therefore contribute to uncertainties in the calculated atmospheric lifetimes of trace species.

For the O_2 cross sections, uncertainties in the Schumann-Runge (S-R) bands (175-205 nm) and the Herzberg continuum (195-242 nm) arise from a combination of uncertainties in the laboratory measurements and the parameterization of the fine wavelength structure and temperature dependence of the S-R bands for use in atmospheric models. Total cross-section uncertainties in the S-R and Herzberg regions are estimated here to be in the range of 10 to 20% (2σ) based on the JPL10-6 data evaluation and Minschwaner *et al*. (2012). The O_3 UV

absorption cross-section uncertainty is taken here to be 4% (2σ), based primarily on the level of agreement among various laboratory measurements.

GSFC 2-D model simulations were used to evaluate the lifetime sensitivity to uncertainties in the O_2 and O_3 UV absorption cross sections. The model utilizes a look-up table calculated with the APL radiative transfer code to obtain the O_2 photolysis and incident solar radiation at each grid point as a function of wavelength (175-847.5 nm), solar zenith angle, overhead ozone column, and pressure (Anderson and Meier, 1979; Swartz *et al*., 1999). For the evaluation of uncertainties, new look-up tables were generated in which the cross sections were increased or decreased by a specified amount and then input into the 2-D model. Uncertainties of both ±10 and ±20% were applied to the O_2 cross sections. Model simulations were first performed with the O_2 cross sections perturbed simultaneously at all wavelengths. However, given the different spectral characteristics of, and atmospheric responses to the S-R and Herzberg regions, model calculations were also performed with the wavelength ranges <204 nm and >204 nm perturbed separately. For O_3, a cross-section uncertainty of ±4% (2σ) was used for all wavelengths, in both the look-up table and 2-D model chemistry. The wavelength bins and base cross sections are provided in the supplementary material. For Lyman-α and the wavelength range 169-175 nm, the O_2 photolysis and incident solar radiation at each grid point are calculated in the 2-D model separately from the look-up table. These wavelength regions have only minor contributions to the total global lifetime of the compounds addressed in this report and are not considered in this uncertainty analysis.

For the species primarily removed in the stratosphere, the lifetime changes due to the perturbations to the absorption cross sections are listed in Table 3.8; species removed primarily in the troposphere are not considered in this analysis since the 2-D model tropospheric OH is specified and therefore does not respond to changes in the O_2 and O_3 cross sections. The percentage change from the baseline case is indicated in parentheses in Table 3.8 (for reference, the baseline lifetimes are repeated from Tables 3.6 and 3.7). In general, reducing the O_2 and O_3 cross sections increases the incident solar flux and photolytic loss, thereby decreasing a compounds' lifetime. Conversely, increasing the cross sections leads to an increased lifetime. For the O_2 cross-section perturbations, the lifetime response is asymmetric for all compounds and wavelength ranges; i.e., reducing the cross sections results in a larger magnitude change (reduction) in lifetime compared with the corresponding response to increasing the cross sections. The magnitude of this asymmetry varies among the different compounds and wavelength ranges.

The results given in Table 3.8 show that since removal of most of the species is dominated by photolytic loss in the stratosphere, there is substantial lifetime sensitivity to uncertainties in the O_2 cross sections. The sensitivity is somewhat less for (1) CFC-115 and NF_3, which have substantial loss due to reaction with $O(^1D)$ and Lyman-α photolysis, and (2) Halon-1202 which has substantial tropospheric photolytic loss at wavelengths >286 nm. The lifetime sensitivity to the uncertainty in the O_3 cross sections (±4%) is small, with changes of less than ±1% for all the compounds. The results in Table 3.8 are based on free-running model simulations in which the O_3 and constituent profiles adjust to the O_2 and O_3 cross-section perturbations. Therefore, the lifetime responses for CFC-11 and CFC-12 are somewhat smaller than reported in Minschwaner *et al*. (2012), who used O_3 and CFC profiles fixed to observations.

The results in Table 3.8 illustrate that the lifetime responses to the O_2 cross-section perturbations are nearly linear; *i.e.*, the ±20% perturbations are roughly twice the magnitude of the ±10% perturbations. This is true for the perturbations made separately above and below 204 nm, and for all wavelength regions perturbed simultaneously. Perturbing the spectral region below 204 nm gives a larger lifetime response for all compounds, compared to perturbing the spectral region above 204 nm. The lifetime responses are combined, assuming the perturbations in the two O_2 wavelength regions and the O_3 perturbation are independent, as

$$\tau_{\text{Perturbed}} = \tau_{\text{Base}} \pm \sqrt{[\tau_{\text{Base}} - \tau_{<204\,nm}^{O_2}]^2 + [\tau_{\text{Base}} - \tau_{>204\,nm}^{O_2}]^2 + [\tau_{\text{Base}} - \tau_{\text{All }\lambda}^{O_3}]^2}$$

where τ_{Base} is the baseline lifetime, $\tau_{<204\,nm}^{O_2}$ and $\tau_{>204\,nm}^{O_2}$ are the lifetimes computed from the separate O_2 cross-section perturbations below and above 204 nm, respectively, and $\tau_{\text{All }\lambda}^{O_3}$ is the lifetime computed with the O_3 cross-section perturbation. The contribution of the O_3 cross-section perturbation to $\tau_{\text{Perturbed}}$ is small due to the weak lifetime sensitivity to the O_3 cross-section uncertainty. For all compounds, the range of $\tau_{\text{Perturbed}}$ is slightly smaller than that obtained from the model calculations with the O_2 cross sections perturbed at all wavelengths simultaneously. For example, for the ±20% O_2 cross-section perturbation for CFC-11, the range of $\tau_{\text{Perturbed}}$ is 49.8–67.8 years, compared to 47.8–70.8 years for all wavelengths perturbed simultaneously. This indicates that responses to the perturbations in the two wavelength regions are not fully independent, i.e., there is a small positive feedback effect present when perturbing the O_2 cross sections at all wavelengths simultaneously.

The recommended overall range in $\tau_{\text{Perturbed}}$ is given in Table 3.8 and was computed using the results from the ±20% O_2 cross-section perturbation below and above 204 nm. The uncertainties given in Table 3.8 as well as the lifetime uncertainties due to the kinetic and photochemical data for each molecule (Table 3.7) are used in Chapter 6 in the determination of the estimated overall lifetime uncertainty for each compound.

3.7 Conclusions and Future Directions

The most critical kinetic and photochemical processes that ultimately determine the atmospheric lifetimes of the compounds included in this report are identified by the fractional contributions and kinetic and photolytic lifetimes as given in Tables 3.6 and 3.7. The uncertainty in the kinetic and photochemical parameters was evaluated (see Tables 3.1 – 3.4 and the Supplementary Material for additional detail for each molecule) and the impact on atmospheric lifetimes was evaluated using 2-D model calculations, see Tables 3.6 and 3.7. Although there are no major gaps in the understanding of the atmospheric processing of these compounds, the 2-D atmospheric model calculations show that the recommended uncertainties in kinetic and photochemical parameters make a non-negligible contribution to the uncertainty (range) in calculated atmospheric lifetimes. The estimated uncertainties given in the SPARC recommendations, in general, lead to a reduction in the range of calculated lifetimes from those calculated using the NASA/JPL (JPL10-6) recommended kinetic parameters. The range in calculated lifetimes obtained for $CFCl_3$ (CFC-11), CF_2Cl_2 (CFC-12), CCl_4, and N_2O using the SPARC recommendations is between 5 and 10% (2σ uncertainty), while for CH_3CCl_3 (methyl chloroform), CH_3Cl, CH_3Br, CHF_2Cl (HCFC-22), and CH_3CCl_2F (HCFC-141b) it is ~20%, and the range is greater for CF_3CClF_2 (CFC-115), CBr_2F_2 (Halon-1202), $CBrClF_2$ (Halon-1211), CH_3CClF_2 (HCFC-142b), and several of the HFCs. Reducing uncertainties in kinetic and photochemical parameters, in general, is

desirable, and the results presented in this chapter and the Supplementary Material can be used to guide the direction of future studies. For example, the extension of rate-coefficient data, in some cases, to the cold temperatures (~200 to 240 K) representative of the UT/LS would help reduce estimated uncertainties in calculated local lifetimes, which are currently based on an extrapolation of kinetic data obtained at higher temperatures. It was also shown that the existing uncertainties in the O_2 absorption cross sections in the Schumann-Runge bands between 190 and 204 nm contribute substantially to the absolute uncertainty in the lifetimes of molecules removed in the stratosphere by UV photolysis, e.g., CFCs. Studies that would reduce the present level of uncertainty in the O_2 absorption cross sections are therefore desired.

Table 3.1. Reaction-rate coefficients and estimated uncertainties for the OH + compound gas-phase reactions.*

Compound	Chemical Formula	Temperature Range (K) **	*A* *	*E*/R (K)	*k*(298 K) *	*f*(298 K)	*g*	Footnotes
1. CFC−11	CCl_3F	–	*10*	*9695*	*<1 (-25)*	_	–	1,2
2. CFC−12	CCl_2F_2	–	*10*	*11910*	*<1 (-28)*	–	–	1,2
3. CFC−113	CCl_2FCClF_2	–	*10*	*>6220*	*<1 (-20)*	–	–	3,4
4. CFC−114	$CClF_2CClF_2$	–	*10*	*>6220*	<1 (-20)	–	–	3,4
5. CFC−115	CF_3CClF_2	–	*10*	*>6220*	*<1 (-20)*	–	–	3,4
6. Carbon Tetrachloride	CCl_4	–	*10*	*6220*	*<1 (-20)*	–	–	1,2
7. Nitrous Oxide	N_2O	–	–	–	*<5.0 (-17)*	–	–	3,a
8. Halon−1202	CBr_2F_2	–	*1*	*>2200*	*<5 (-16)*	–	–	5
9. Halon−1211	$CBrClF_2$	–	*1*	*>3500*	*<8 (-18)*	–	–	2,b
10. Halon−1301	$CBrF_3$	–	*1*	*>3600*	*<6 (-18)*	–	–	5
11. Halon−2402	$CBrF_2CBrF_2$	–	*1*	*>3600*	*<6 (-18)*	–	–	5
12. Methane	CH_4	195 – 300	1.85	1690	6.4 (-15)	1.05	50	2,c
13. Methyl Chloroform	CH_3CCl_3	233 – 379	1.64	1520	1.0 (-14)	1.10	50	5,6
14. Methyl Chloride	CH_3Cl	224 – 298	1.96	1200	3.5 (-14)	1.10	50	2,6,d
15. Methyl Bromide	CH_3Br	233 – 300	1.40	1150	3.0 (-14)	1.07	100	2,6,e
16. HCFC−22	$CHClF_2$	250 – 391	1.03	1600	4.8 (-15)	1.07	100	2,6
17. HCFC−141b	CH_3CCl_2F	250 – 400	1.25	1600	5.8 (-15)	1.07	100	5,6,f
18. HCFC−142b	CH_3CClF_2	223 – 400	1.30	1770	3.4 (-15)	1.15	50	5,6
19. HFC−23	CHF_3	252 – 298	0.52	2210	3.1 (-16)	1.15	100	5
20. HFC−32	CH_2F_2	222 – 384	1.70	1500	1.1 (-14)	1.07	100	5,6
21. HFC−125	CHF_2CF_3	220 – 364	0.60	1700	2.0 (-15)	1.10	100	5,6,g
22. HFC−134a	CH_2FCF_3	223 – 400	0.95	1600	4.4 (-15)	1.10	100	2,6,h
23. HFC−143a	CF_3CH_3	261 – 403	1.06	2010	1.25 (-15)	1.10	100	2,i
24. HFC−152a	CH_3CHF_2	210 – 300	0.87	975	3.3 (-14)	1.05	50	5,6,j
25. HFC−227ea	CF_3CHFCF_3	250 – 400	0.48	1680	1.7 (-15)	1.15	75	2,6,k
26. HFC−245fa	$CHF_2CH_2CF_3$	273 – 370	0.61	1330	7.0 (-15)	1.15	100	5,6
27. Nitrogen Trifluoride	NF_3	–	*10*	*>17500*	*<3 (-37)*	–	–	1,3,l

Footnotes

* Estimated values are given in italics; A is in units of 10^{-12} cm^3 molecule^{-1} s^{-1}; k(298 K) is in units of cm^3 molecule^{-1} s^{-1} and (-xx) represents $\times 10^{-xx}$; $k(T) = A \exp(-E/RT)$.

** Temperature range of available experimental data considered in the evaluation of the reaction-rate coefficient parameters and uncertainty limits.

1 The recommendation given here was obtained by setting the pre-exponential factor (A) to 1×10^{-11} cm^3 molecule^{-1} s^{-1} and equating the activation energy (E) to the reaction endothermicity using the thermochemical parameters reported in JPL10-6 and IUPAC. The JPL10-6 recommendation was derived from experimentally determined rate-coefficient upper limits.

2 A and/or E/R recommendation is revised from JPL10-6.

3 Not evaluated in JPL10-6.

4 The recommended kinetic parameters are taken to be equal to those for the OH + CCl_4 reaction.

5 A and E/R recommendation is unchanged from JPL10-6.

6 f(298 K) and/or g is revised from JPL10-6.

a Based on the study by Biermann *et al.* (1976), who measured a rate coefficient of 3.8×10^{-17} cm^3 molecule^{-1} s^{-1} at 298 K. A more conservative upper limit (4.0×10^{-16} cm^3 molecule^{-1} s^{-1}) was reported by Chang and Kaufman (1977b).

b Rate-coefficient expression was estimated using an estimated Arrhenius A-factor and the rate-coefficient upper limit reported by Burkholder *et al.* (1991) at 373 K.

c A and/or E/R recommendation was taken from IUPAC data evaluation.

d The recommended k(298 K) was obtained from an average of the data of Hsu and DeMore (1994), Orkin *et al.* (2013), and Herndon *et al.* (2001). The recommended E/R was obtained from a fit to the data of Herndon *et al.* below 298 K.

e The recommended k(298 K) was obtained from an average of the data of Hsu and DeMore (1994) (recalculated based on the JPL10-6-recommended rate coefficient for the OH + CH_3CHF_2 reference reaction), Chichinin *et al.* (1994), Mellouki *et al.* (1992), and Zhang *et al.* (1992). The recommended value for E/R was derived from a fit to the data of Mellouki *et al.* below 300 K.

f The data from Lancar *et al.* (1993) at T<400K were used in the fit to obtain E/R.

g The recommended k(298 K) was obtained from an average of the data of Talukdar *et al.* (1991), DeMore (1993), and Young *et al.* (2009). The recommended value for E/R was taken from Talukdar *et al.*

h The present analysis differs from that given in JPL10-6 in that the three rate coefficients reported in DeMore (1993) were averaged in the determination of E/R.

i The present analysis differs from that given in JPL10-6 in that the DF-LMR results of Talukdar *et al.* (1991) were not included in the analysis for k(298K), although their LP-LIF results were included.

j The site-specific rate coefficients were estimated by Kozlov *et al.* (2003) to be 33% reaction at the CH_3 group and 67% H atom abstraction from the CH_2F group.

k The recommended k(298 K) was obtained from an average of the results from the absolute-rate studies of Nelson *et al.* (1993), Zellner *et al.* (1994), Zhang *et al.* (1994), and Tokuhashi *et al.* (2004) and the relative-rate studies of Hsu and DeMore (1995) (recalculated based on the JPL10-6-recommended rate coefficients for the OH + CH_4 and OH + CHF_2CF_3 reference reactions) and Wallington *et al.* (2004) (recalculated based on the JPL10-6-recommended rate coefficient for the OH + C_2H_4 and OH + C_2H_2 reference reactions). The recommended value for E/R was based on a fit of the data below 400 K from Nelson *et al.* (1993), Zellner *et al.* (1994), Tokuhashi *et al.* (2004), and Hsu and DeMore (1995) after scaling to the recommended k(298 K) value.

l The rate-coefficient parameters were estimated using a G3B3 quantum chemical method (Curtiss *et al.*, 2001) calculation of the reaction activation barrier, ~146 kJ mol^{-1}. Assuming a pre-exponential factor of 1×10^{-11} cm^3 $molecule^{-1}$ s^{-1} and E/R equal to the calculated activation barrier provides the basis of the recommendation.

Table 3.2. Reaction-rate coefficients, reaction yields, and estimated uncertainties for the $O(^1D)$ + compound gas-phase reactions.*

Compound	Chemical Formula	Temperature Range (K) **	*A* *	*E*/R (K)	*k*(298 K) *	*f*(298 K)	*g*	Reaction Yield	Footnotes
1. CFC−11	CCl_3F	173 – 372	230	0	230	1.10	0	0.79 ± 0.04	1,2,3
2. CFC−12	CCl_2F_2	173 – 373	140	-25	157	1.15	0	0.76 ± 0.06	1,2,3,4
3. CFC−113	CCl_2FCClF_2	217 – 373	232	0	232	1.1	0	0.80 ± 0.04	2,3,4,5
4. CFC−114	$CClF_2CClF_2$	217 – 373	130	-25	142	1.1	0	0.80 ± 0.10	2,3,4,5
5. CFC−115	CF_3CClF_2	217 – 373	54	-30	60	1.15	0	0.84 ± 0.07	2,3,4
6. Carbon Tetrachloride	CCl_4	203 – 343	330	0	330	1.15	0	0.79 ± 0.04	1,2
7. Nitrous Oxide	N_2O	195 – 719	119	-20	127	1.1	25	0.39 (N_2 + O_2) 0.61 (2NO)	6
8. Halon−1202	CBr_2F_2	297	220	*0*	220	1.2	50	0.45 ± 0.06	6
9. Halon−1211	$CBrClF_2$	297	150	*0*	150	1.2	50	0.65 ± 0.04	6
10. Halon−1301	$CBrF_3$	297	100	*0*	100	1.2	50	0.40 ± 0.08	6
11. Halon−2402	$CBrF_2CBrF_2$	297	160	*0*	160	1.2	50	0.75 ± 0.07	6
12. Methane	CH_4	198 – 369	175	0	175	1.15	25	$1.0^{+0}_{-0.002}$	6
13. Methyl Chloroform	CH_3CCl_3	298	*325*	*0*	*325*	1.4	*0*	*0.9*	7,8
14. Methyl Chloride	CH_3Cl	298	260	*0*	260	1.3	50	0.91 ± 0.06	7,9
15. Methyl Bromide	CH_3Br	297	180	*0*	180	1.15	50	$1.0^{+0}_{-0.07}$	6
16. HCFC−22	$CHClF_2$	173 – 373	102	0	102	1.07	0	0.72 ± 0.06	2,3,4
17. HCFC−141b	CH_3CCl_2F	297	260	*0*	260	1.2	50	0.70 ± 0.05	6
18. HCFC−142b	CH_3CClF_2	217 – 373	200	0	200	1.1	0	0.75 ± 0.05	2,3,4
19. HFC−23	CHF_3	217 –372	8.7	-30	9.6	1.05	0	0.25 ± 0.05	2,3,4
20. HFC−32	CH_2F_2	298	51	*0*	51	1.2	50	0.30 ± 0.10	6
21. HFC−125	CHF_2CF_3	217 – 373	9.5	-25	10.5	1.07	0	0.70 ± 0.09	2,4,10
22. HFC−134a	CH_2FCF_3	297	49	*0*	49	1.15	50	0.35 ± 0.06	6
23. HFC−143a	CF_3CH_3	217 – 373	56	-20	60	1.2	0	0.65 ± 0.05	2,3,4
24. HFC−152a	CH_3CHF_2	297	175	*0*	175	1.2	50	0.55 ± 0.20	6
25. HFC−227ea	CF_3CHFCF_3	217 – 373	7.9	-70	10	1.1	0	0.72 ± 0.07	7,10
26. HFC−245fa	$CHF_2CH_2CF_3$	–	*150*	*0*	*150*	*1.3*	*0*	*0.5*	7
27. Nitrogen Trifluoride	NF_3	212 – 351	*20*	-44	*23*	*1.1*	*0*	$0.93^{+0.07}_{-0.21}$	2,4,11

Footnotes

* Estimated values are given in italics; A and k(298 K) are in units of 10^{-12} cm^3 $molecule^{-1}$ s^{-1}; $k(T) = A \exp(-E/RT)$.

** Temperature range of available experimental data considered in the evaluation of the reaction-rate coefficient parameters and uncertainty limits.

1. Reactive yields taken from Feierabend *et al.* (2010).
2. Estimated uncertainty parameters revised from values reported in JPL10-6.
3. Recommended kinetic parameters and uncertainties based on evaluation of studies included in JPL10-6 as well as Baasandorj *et al.* (2013).
4. Kinetic parameters revised from values reported in JPL10-6.
5. Kinetic parameters taken from Baasandorj *et al.* (2011) and Baasandorj *et al.* (2013).
6. Kinetic parameters taken from JPL10-6.
7. Not evaluated in JPL10-6.
8. Nilsson *et al.* (2012) report a room-temperature reactive-rate coefficient, obtained using a relative-rate method, of $(2.93 \pm 1.2) \times 10^{-10}$ cm^3 $molecule^{-1}$ s^{-1} (1σ error limit). The total rate coefficient given in the table was calculated assuming a 0.9 reaction yield.
9. Rate coefficient is an average of the values reported by Matsumi *et al.* (1993) and Force and Wiesenfeld (1981). The reaction yield was taken from Force and Wiesenfeld (1981).
10. Kinetic parameters taken from Baasandorj *et al.* (2013).
11. The recommended k(298 K) for the overall reaction is an average of the values derived from Arrhenius fits to the data of Zhao *et al.* (2010) and Dillon *et al.* (2011) and the value reported by Baasandorj *et al.* (2012) at 296 K. The recommended Arrhenius parameters are derived from a fit to these data after normalization to k(298 K). The recommended reaction yield is an average of the values reported by Zhao *et al.* (0.99) and Baasandorj *et al.* (2012) (0.87 +0.13/-0.15). The reaction yield is expected to be independent of temperature.

Table 3.3. Reaction-rate coefficients and estimated uncertainties for the Cl + compound gas-phase reactions.*

Compound	Chemical Formula	Temperature Range (K) **	*A* *	*E*/R (K)	*k*(298 K) *	*f*(298 K)	*g*	Footnotes
1. CFC−11	CCl_3F	–	*100*	*8960*	*<8.7 (-24)*	–	–	1
2. CFC−12	CCl_2F_2	–	*100*	*11100*	*<5.2 (-27)*	–	–	1
3. CFC−113	CCl_2FCClF_2	–	*100*	*>5480*	*<1.0 (-18)*	–	–	2
4. CFC−114	$CClF_2CClF_2$	–	*100*	*>5480*	*<1.0 (-18)*	–	–	2
5. CFC−115	CF_3CClF_2	–	*100*	*>5480*	*<1.0 (-18)*	–	–	2
6. Carbon Tetrachloride	CCl_4	–	*100*	*5480*	*<1.0 (-18)*	–	–	1
7. Nitrous Oxide	N_2O	–	–	–	<1 (-17)			3
8. Halon−1202	CBr_2F_2	–	*100*	*9320*	*<2.6 (-24)*	–	–	1,a
9. Halon−1211	$CBrClF_2$	–	*100*	*6280*	*<7.1 (-20)*	–	–	1
10. Halon−1301	$CBrF_3$	–	*100*	*9290*	*<2.9 (-24)*	–	–	1
11. Halon−2402	$CBrF_2CBrF_2$	–	*100*	*9320*	*<2.6 (-24)*	–	–	1,a
12. Methane	CH_4	181 – 300	7.3	1280	1.0 (-13)	1.05	50	3
13. Methyl Chloroform	CH_3CCl_3	253 – 418	2.86	1716	9.03 (-15)	1.10	100	4,5,b
14. Methyl Chloride	CH_3Cl	222 – 300	19	1100	4.80 (-13)	1.07	50	4,5,c
15. Methyl Bromide	CH_3Br	213 – 300	14	1030	4.40 (-13)	1.05	50	3
16. HCFC−22	$CHClF_2$	298 – 430	5.57	2430	1.60 (-15)	1.08	100	3,5
17. HCFC−141b	CH_3CCl_2F	295 – 429	2.76	2140	2.10 (-15)	1.10	200	4,5,d
18. HCFC−142b	CH_3CClF_2	295 – 429	1.40	2420	4.10 (-16)	1.08	200	4,5,e
19. HFC−23	CHF_3	–	–	–	<5.0 (-16)	–	–	3
20. HFC−32	CH_2F_2	253 – 318	6.93	1590	3.34 (-14)	1.08	100	4,5,f
21. HFC−125	CHF_2CF_3	298	*1.8*	*2600*	3.0 (-16)	1.25	300	3,5
22. HFC−134a	CH_2FCF_3	253 – 300	0.98	1953	1.40 (-15)	1.10	200	4,g
23. HFC−143a	CF_3CH_3	281 – 368	9.7	3760	3.20 (-17)	2	300	4,5,h
24. HFC−152a	CH_3CHF_2	264 – 360	6.3	965	2.5 (-13)	1.10	100	4,i
25. HFC−227ea	CF_3CHFCF_3	298	*2.7*	*2600*	4.39 (-16)	1.30	300	j
26. HFC−245fa	$CHF_2CH_2CF_3$	298	*2.1*	*1700*	6.90 (-15)	1.30	300	k
27. Nitrogen Trifluoride	NF_3	–	*100*	*13200*	<1 (-29)	–	–	1,l

Footnotes

* Estimated values are given in italics; A is in units of 10^{-12} cm^3 molecule^{-1} s^{-1}; k(298 K) is in units of cm^3 molecule^{-1} s^{-1} and (-xx) represents $\times 10^{-xx}$; $k(T) = A \exp(-E/RT)$.

** Temperature range of available experimental data considered in the evaluation of the reaction-rate coefficient parameters and uncertainty limits.

1 No experimental data available for this reaction. The reaction was not evaluated in JPL10-6. The recommendation given here was obtained by setting the pre-exponential factor (A) to 1×10^{-10} cm^3 molecule^{-1} s^{-1} and equating the activation energy (E) to the reaction endothermicity using the thermochemical parameters reported in JPL10-6 and IUPAC.

2 The recommended kinetic parameters are taken to equal those for the Cl + CCl_4 reaction.

3 A and E/R recommendation is unchanged from JPL10-6.

4 A and E/R recommendation is revised from JPL10-6.

5 f(298 K) and/or g is revised from JPL10-6.

a The rate-coefficient upper limit was estimated with E = 77.5 kJ mol^{-1}, which was obtained from an average of the values for the reaction of Cl with CH_3Br (77.8 kJ mol^{-1}) and CF_3Br (77.2 kJ mol^{-1}).

b The recommended k(298 K) was obtained from an average of the results from the relative-rate studies of Platz *et al.* (1995) and Nilsson *et al.* (2009) and the absolute-rate study of Talhaoui *et al.* (1996). The rate-coefficient temperature dependence was obtained from a fit of the data from Talhaoui *et al.* (1996) and Nilsson *et al.* (2009) after scaling to the recommended k(298 K) value.

c The recommended k(298 K) is an average of the results from Manning and Kurylo (1977), Wallington *et al.* (1990), Beichert *et al.* (1995), Orlando (1999), and Bryukov *et al.* (2002). The rate-coefficient temperature dependence was obtained from a fit of the data from Manning and Kurylo (1977), Wallington *et al.* (1990), Beichert *et al.* (1995), Orlando (1999), Bryukov *et al.* (2002), and Sarzyński *et al.* (2009) for temperatures <300 K.

d The recommended k(298 K) is an average of the results from Wallington and Hurley (1992), Tuazon *et al.*, (1992), Warren and Ravishankara (1993), and Talhaoui *et al.* (1996). The rate-coefficient temperature dependence is based on a fit of the results from the studies of Warren and Ravishankara (<350 K) and Talhaoui *et al.* after scaling to the recommended k(298 K) value.

e The recommended k(298 K) is an average of the results from Wallington and Hurley (1992), Tuazon *et al.* (1992), and Talhaoui *et al.* (1996). The rate-coefficient temperature dependence was taken from Talhaoui *et al.* (1996), which is the only available temperature-dependent study.

f The recommended k(298 K) is an average of the results from Nielsen *et al.* (1992) and Nilsson *et al.* (2009). The rate-coefficient temperature dependence was obtained from a fit of the data from Nielsen *et al.* (1992) and Nilsson *et al.* (2009) for temperatures <300 K after scaling to the recommended k(298 K) value.

g The recommended k(298 K) is an average of the data from Louis *et al.* (1997), Wallington and Hurley (1992), Tuazon *et al.* (1992), Kaiser (1993), and Nilsson *et al.*

(2009). The rate-coefficient temperature dependence was obtained by fitting the T <300 K data from Louis *et al.* (1997), Kaiser (1993), and Nilsson *et al.* (2009) after scaling to match the recommended *k*(298 K) value.

h The recommended *k*(298 K) is an average of the results from the Tschuikow-Roux *et al.* (1985) and Nielsen *et al.* (1994) relative-rate studies. The rate-coefficient temperature dependence is based on the work of Tschuikow-Roux *et al.* (1985) combined with the rate expression for the Cl + CH_4 reaction recommended in this report.

i The recommended *A* and *E*/R values are for the total rate coefficient, i.e., loss of HFC-152a. The recommended *k*(298 K) was obtained from an average of one absolute-rate and four relative-rate studies, which are in good agreement. The temperature dependence was taken from Yano and Tschuikow-Roux (1986) where the site-specific rate coefficients are given as

$Cl + CH_3CHF_2 \rightarrow HCl + CH_3CF_2$; $k(T) = 6.3 \times 10^{-12} \exp(-965/T)$ cm^3 molecule^{-1} s^{-1}

$Cl + CH_3CHF_2 \rightarrow HCl + CH_2CHF_2$; $k(T) = 7.0 \times 10^{-12} \exp(-2400/T)$ cm^3 molecule^{-1} s^{-1}

j The recommended *k*(298 K) is the average of the relative-rate determinations by Møgelberg *et al.* (1996) and *E*/R was estimated by comparison with compounds having similar reactivity at 298 K (e.g., HFC-125). The reaction was not evaluated in JPL10-6.

k The recommended *k*(298 K) was taken from Chen *et al.* (1997) and *E*/R was estimated by comparison with compounds having similar reactivity at 298 K (e.g., CH_3CCl_3). The reaction was not evaluated in JPL10-6.

l F atom abstraction from NF_3 by Cl is slightly exothermic (Gurvich *et al.*, 1989), ca. -11 kJ mol^{-1}. A G3B3 quantum chemical method (Curtiss *et al.*, 2001) calculation predicts an activation barrier (*E*/R) of ~110 kJ mol^{-1} for this reaction. Assuming a pre-exponential factor (*A*) of 1×10^{-10} cm^3 molecule^{-1} s^{-1} and this activation barrier provides the basis for the recommendation.

Table 3.4. Summary of Lyman-α (121.567 nm) absorption cross sections, σ(L-α), at 298 K and estimated cross-section value uncertainties at Lyman-α and in the 169- to 190-, 190- to 230-, 230- to 286-, and >286-nm wavelength regions. *

Compound	Chemical Formula	Lyman-α (121.567 nm)		*p*(298 K)/*w*				Footnotes
		σ(L-α, 298 K)**	*p*(298 K)	169-190 nm	190-230 nm	230-286 nm	>286 nm	
1. CFC−11	CCl_3F	9.8	1.2	1.10/60	1.10/120	1.30/–	–/–	1
2. CFC−12	CCl_2F_2	2.07	1.15	1.10/40	1.08/40	1.30/–	–/–	1
3. CFC−113	CCl_2FCClF_2	10	2.0	1.10/120	1.06/120	1.20/–	–/–	2
4. CFC−114	$CClF_2CClF_2$	3.6	1.3	1.14/60	1.14/60	–/–	–/–	1
5. CFC−115	CF_3CClF_2	0.457	3.0	1.14/–	1.30/–	–/–	–/–	1
6. Carbon Tetrachloride	CCl_4	3.7	1.2	1.10/120	1.06/60	1.20/–	–/–	3
7. Nitrous Oxide	N_2O	2.4	1.5	1.12/60	1.08/20	1.12/–	1.30/–	1
8. Halon−1202	CBr_2F_2	10	1.5	1.08/120	1.08/120	1.14/120	1.20/220	4
9. Halon−1211	$CBrClF_2$	7.75	1.5	1.10/500	1.10/500	1.14/220	1.40/220	4
10. Halon−1301	$CBrF_3$	2.5	1.4	1.16/220	1.08/120	1.20/120	1.30/–	1
11. Halon−2402	$CBrF_2CBrF_2$	*5*	2.0	1.14/120	1.10/120	1.14/60	1.30/220	4
12. Methane	CH_4	1.85	1.3	–/–	–/–	–/–	–/–	5,6
13. Methyl Chloroform	CH_3CCl_3	*7*	1.4	1.18/60	1.18/120	1.18/120	–/–	1
14. Methyl Chloride	CH_3Cl	8.8	1.15	1.06/60	1.12/120	1.24/–	–/–	1
15. Methyl Bromide	CH_3Br	3.2	1.3	1.06/60	1.06/60	1.10/60	–/–	1
16. HCFC−22	$CHClF_2$	1.76	1.4	1.10/30	1.26/60	–/–	–/–	1
17. HCFC−141b	CH_3CCl_2F	6.6	2.0	1.12/120	1.12/120	–/–	–/–	1
18. HCFC−142b	CH_3CClF_2	3.1	1.2	1.20/120	1.14/120	–/–	–/–	1
19. HFC−23	CHF_3	0.035	2.0	–/–	–/–	–/–	–/–	5,6
20. HFC−32	CH_2F_2	0.55	1.4	–/–	–/–	–/–	–/–	5
21. HFC−125	CHF_2CF_3	*0.035*	3.0	–/–	–/–	–/–	–/–	5
22. HFC−134a	CH_2FCF_3	*0.5*	2.0	–/–	–/–	–/–	–/–	6
23. HFC−143a	CF_3CH_3	1.75	2.0	–/–	–/–	–/–	–/–	5,6
24. HFC−152a	CH_3CHF_2	3.2	2.0	–/–	–/–	–/–	–/–	5
25. HFC−227ea	CF_3CHFCF_3	*0.035*	3.0	–/–	–/–	–/–	–/–	5
26. HFC−245fa	$CHF_2CH_2CF_3$	*1*	3.0	–/–	–/–	–/–	–/–	5
27. Nitrogen Trifluoride	NF_3	0.48	1.5	1.5/–	1.1/–	1.5/–	–/–	5

Footnotes

* p(298 K) and w are 2σ (95% confidence level) values where the uncertainty at temperature T (K) is given by $p(T) = p(298\ K)\exp(|w(1/T - 1/298)|)$.

** Absorption cross sections are in units of 10^{-17} cm^2 $molecule^{-1}$; estimated values are given in italics

1 The recommended cross sections and their wavelength and temperature parameterization are taken from JPL 10-6.

2 The absorption cross-section wavelength and temperature parameterization reported in JPL10-6 contains an error; a revised set of parameters was derived here.

3 The cross-section wavelength and temperature parameterization reported in JPL10-6 has been revised to include the parameterization between 200-230 nm reported in Rontu *et al.* (2010).

4 The recommended absorption cross sections at $\lambda \geq 260$ nm are based on the parameterizations given in Papanastasiou *et al.* (2013).

5 Not included in JPL10-6 evaluation.

6 No UV spectral data are available. Photolysis at wavelengths >169 nm is expected to make a negligible contribution to the molecule's atmospheric loss.

Table 3.5. Summary of 2-D model simulations for year 2000 steady-state conditions.

Simulation	Input Kinetic and Photolytic Parameters	Model Conditions[a,b,c]
A	JPL10-6	Baseline
B	JPL10-6	2σ slow for all, interactive
C	JPL10-6	2σ fast for all, interactive
D	JPL10-6	2σ slow for all, non-interactive tracers
E	JPL10-6	2σ slow for all, non-interactive tracers
F	SPARC	Baseline
G	SPARC	2σ slow for all, interactive
H	SPARC	2σ fast for all, interactive
I	SPARC	2σ slow for CH_4 kinetics, Baseline for others, interactive
J	SPARC	2σ fast for CH_4 kinetics, Baseline for others, interactive
K	SPARC	2σ slow for N_2O kinetics and photolysis, Baseline for others, interactive
L	SPARC	2σ slow for N_2O kinetics and photolysis, Baseline for others, interactive
M	SPARC	2σ slow for all, non-interactive tracers
N	SPARC	2σ fast for all, non-interactive tracers
O	SPARC	2σ slow for all $O(^1D)$ reactions, 2σ fast for all photolysis, non-interactive tracers
P	SPARC	2σ fast for all $O(^1D)$ reactions, 2σ slow for all photolysis, non-interactive tracers

[a] all ≡ the kinetic and photolysis parameters for the compounds reported in this chapter (Tables 3.1 – 3.4)

[b] interactive ≡ the compounds allowed to interact with the other model constituents including ozone

[c] non-interactive ≡ the compounds treated as non-interactive tracers

Table 3.6. Fractional loss contributions and global annually averaged atmospheric lifetimes calculated using a 2-D model for 2000 steady-state conditions.*

Compound	Formula	hν (121.56 nm)	hν (169-190 nm)	hν (190-230 nm)	hν (230-286 nm)	hν (>286 nm)	hν Total	$O(^1D)$ Reactive Loss	OH Reaction	Cl Reaction	Lifetime (Years)
1. CFC−11	CCl_3F	<0.001	0.002	0.981	<0.001	–	0.982	0.018	–	–	60.2
		(–)	(0.001)	(0.977)	(<0.001)	(–)	(0.979)	(0.019)	(0.002)	(–)	(58.6)
2. CFC−12	CCl_2F_2	<0.001	0.029	0.913	<0.001	–	0.942	0.058	–	–	109.5
		(–)	(0.024)	(0.919)	(<0.001)	(–)	(0.943)	(0.051)	(0.006)	(–)	(103.7)
3. CFC−113	CCl_2FCClF_2	<0.001	0.013	0.930	<0.001	–	0.942	0.058	<0.001	<0.001	93.6
		(–)	(0.013)	(0.920)	(<0.001)	(–)	(0.933)	(0.067)	(–)	(–)	(95.4)
4. CFC−114	$CClF_2CClF_2$	0.008	0.055	0.654	–	–	0.717	0.283	<0.001	<0.001	199.7
		(–)	(0.059)	(0.692)	(<0.001)	(–)	(0.751)	(0.249)	(–)	(–)	(204.2)
5. CFC−115	CF_3CClF_2	0.063	0.028	0.283	–	–	0.374	0.626	<0.001	<0.001	539.9
		(–)	(0.062)	(0.573)	(–)	(–)	(0.635)	(0.365)	(–)	(–)	(960.7)
6. Carbon Tetrachloride	CCl_4	<0.001	<0.001	0.983	–	–	0.983	0.017	–	–	48.7
		(–)	(<0.001)	(0.749)	(<0.001)	(–)	(0.749)	(0.015)	(0.236)	(–)	(38.0)
7. Nitrous Oxide	N_2O	<0.001	0.012	0.888	<0.001	–	0.901	0.099	–	–	125.2
		(–)	(0.012)	(0.889)	(–)	(–)	(0.901)	(0.099)	(–)	(–)	(125.2)
8. Halon−1202	CBr_2F_2	<0.001	<0.001	0.057	<0.001	0.920	0.977	<0.001	0.023	<0.001	2.54
		(–)	(<0.001)	(0.042)	<0.001	(0.939)	(0.981)	(<0.001)	(0.019)	(–)	(2.09)
9. Halon−1211	$CBrClF_2$	<0.001	<0.001	0.419	<0.001	0.578	0.997	0.002	0.001	<0.001	16.3
		(–)	(<0.001)	(0.344)	(<0.001)	(0.627)	(0.970)	(0.001)	(0.029)	(–)	(13.5)
10. Halon−1301	$CBrF_3$	<0.001	<0.001	0.986	<0.001	0.002	0.988	0.007	0.005	<0.001	77.4
		(–)	(<0.001)	(0.986)	(<0.001)	(0.002)	(0.988)	(0.007)	(0.005)	(–)	(77.4)
11. Halon−2402	$CBrF_2CBrF_2$	<0.001	<0.001	0.724	<0.001	0.271	0.995	0.003	0.002	<0.001	27.8
		(–)	(<0.001)	(0.349)	(<0.001)	(0.648)	(0.997)	(0.002)	(0.001)	(–)	(13.9)
12. Methane	CH_4	<0.001	–	–	–	–	<0.001	0.019	0.966	0.015	9.32
		<0.001	(–)	(–)	(–)	(–)	(<0.001)	(0.019)	(0.965)	(0.016)	(9.56)
13. Methyl Chloroform	CH_3CCl_3	<0.001	<0.001	0.091	<0.001	–	0.091	<0.001	0.909	<0.001	5.19
		(–)	(<0.001)	(0.097)	(<0.001)	(–)	(0.097)	(–)	(0.903)	(<0.001)	(5.15)
14. Methyl Chloride	CH_3Cl	<0.001	<0.001	0.002	<0.001	–	0.003	0.001	0.991	0.005	1.47
		(–)	(<0.001)	(0.003)	(<0.001)	(–)	(0.003)	(–)	(0.992)	(0.005)	(1.45)
15. Methyl Bromide	CH_3Br	<0.001	<0.001	0.031	<0.001	<0.001	0.031	<0.001	0.966	0.003	1.65
		(–)	(<0.001)	(0.033)	(<0.001)	(<0.001)	(0.033)	(<0.001)	(0.964)	(0.003)	(1.70)
16. HCFC−22	$CHClF_2$	0.002	<0.001	0.002	–	–	0.004	0.014	0.982	<0.001	12.2
		(–)	(<0.001)	(0.002)	(–)	(–)	(0.003)	(0.013)	(0.984)	(<0.001)	(12.0)
17. HCFC−141b	CH_3CCl_2F	<0.001	0.001	0.093	<0.001	–	0.094	0.005	0.902	<0.001	9.2
		(–)	(0.001)	(0.093)	(<0.001)	(–)	(0.094)	(0.004)	(0.902)	(<0.001)	(9.20)
18. HCFC−142b	CH_3CClF_2	0.002	0.001	0.011	–	–	0.014	0.037	0.949	<0.001	17.5
		(–)	(0.001)	(0.011)	(–)	(–)	(0.012)	(0.041)	(0.947)	(<0.001)	(17.5)
19. HFC−23	CHF_3	0.005	–	–	–	–	0.005	0.015	0.980	–	223.8
		(–)	(–)	(–)	(–)	(–)	(–)	(0.009)	(0.991)	(–)	(226.4)
20. HFC−32	CH_2F_2	<0.001	–	–	–	–	<0.001	0.001	0.997	0.002	5.21
		(–)	(–)	(–)	(–)	(–)	(–)	(0.001)	(0.997)	(0.002)	(5.21)
21. HFC−125	CHF_2CF_3	<0.001	–	–	–	–	–	0.005	0.994	<0.001	30.6
		(–)	(–)	(–)	(–)	(–)	(–)	(0.050)	(0.950)	(<0.001)	(29.3)
22. HFC−134a	CH_2FCF_3	0.001	–	–	–	–	0.001	0.004	0.994	<0.001	13.4
		(–)	(–)	(–)	(–)	(–)	(–)	(0.004)	(0.996)	(<0.001)	(13.6)
23. HFC−143a	CF_3CH_3	0.014	–	–	–	–	0.014	0.045	0.941	<0.001	51.0
		(–)	(–)	(–)	(–)	(–)	(–)	(0.041)	(0.959)	(<0.001)	(50.1)
24. HFC−152a	CH_3CHF_2	<0.001	–	–	–	–	<0.001	0.001	0.996	0.003	1.45
		(–)	–)	(–	(–)	(–)	(–)	(0.001)	(0.997)	(0.002)	(1.45)
25. HFC−227ea	CF_3CHFCF_3	0.001	–	–	–	–	0.001	0.005	0.994	<0.001	35.6
		(–)	(–)	(–)	(–)	(–)	(–)	(–)	(1.0)	(–)	(42.3)
26. HFC−245fa	$CHF_2CH_2CF_3$	<0.001	–	–	–	–	<0.001	0.008	0.991	0.001	7.73
		(–)	(–)	(–)	(–)	(–)	(–)	(–)	(1.0)	(–)	(7.79)
27. Nitrogen Trifluoride	NF_3	0.063	0.100	0.549	0.001	0	0.713	0.287	–	–	569.2
		(–)	(–)	(–)	(–)	(–)	(–)	(1.0)	(–)	(–)	(1588)

* Model input kinetic and photochemical parameters from the present SPARC evaluation. The values obtained using the JPL10-6 evaluation parameters as model input are given in parenthesis.

Table 3.7. Summary of global annually averaged atmospheric lifetimes (years) calculated using a 2-D model for 2000 steady-state conditions.*

Compound	Formula	Lifetime (Total)	Lifetime Range **	% Range in Lifetime	Tropospheric	Stratospheric	Mesospheric
1. CFC−11	CCl_3F	60.2	54.3-66.3	± 10	1718	62.4	>1e6
		(58.6)	(54.5-62.8)	(± 7)	(1482)	(61.0)	(>1e6)
2. CFC−12	CCl_2F_2	109.5	102.9-116.1	± 6.0	9879	110.8	196500
		(103.7)	(96.6-110.7)	(± 7)	(5944)	(105.6)	(394400)
3. CFC−113	CCl_2FCClF_2	93.6	86.6-100.7	± 7.5	5708	95.1	>1e6
		(95.4)	(90.4-98.4)	(± 4)	(5661)	(97.1)	(>1e6)
4. CFC−114	$CClF_2CClF_2$	199.7	178.3-223.9	± 11	15540	218.4	2743
		(204.2)	(186.1-217.8)	(± 8)	(18160)	(222.5)	(2878)
5. CFC−115	CF_3CClF_2	539.9	414.8-717.1	± 28	37420	664.4	3119
		(960.7)	(762-1144)	(± 20)	(1.24e5)	(1158)	(5914)
6. Carbon Tetrachloride	CCl_4	48.7	45.2-52.3	± 7.3	885.9	51.6	>1e6
		(38.0)	(35.6-40.3)	(± 6)	(137.7)	(52.4)	(>1e6)
7. Nitrous Oxide	N_2O	125.2	118.1-132.3	± 5.7	10990	127.5	19250
		(125.2)	(113.0-139.6)	(± 11)	(11010)	(127.5)	(19360)
8. Halon−1202	CBr_2F_2	2.54	1.96-3.26	± 26	2.74	35.9	>1e6
		(2.09)	(0.53-7.50)	(± 167)	(2.26)	(27.8)	(>1e6)
9. Halon−1211	$CBrClF_2$	16.3	10.8-23.8	± 40	27.2	40.9	>1e6
		(13.5)	(4.18-34.0)	(± 110)	(20.3)	(40.1)	(>1e6)
10. Halon−1301	$CBrF_3$	77.4	70.9-84.0	± 8.5	3343	79.3	>1e6
		(77.4)	(67.7-87.9)	(± 13)	(3338)	(79.3)	(>1e6)
11. Halon−2402	$CBrF_2CBrF_2$	27.8	22.9-33.3	± 19	85.5	41.3	>1e6
		(13.9)	(4.32-36.4)	(± 115)	(22.5)	(36.6)	(>1e6)
12. Methane	CH_4	9.32	8.17-10.6	± 13	9.92	159.6	4223
		(9.56)	(7.43-12.2)	(± 25)	(10.2)	(163.3)	(4168)
13. Methyl Chloroform	CH_3CCl_3	5.19	4.17-6.44	± 22	5.76	53.1	>1e6
		(5.15)	(3.76-6.97)	(± 31)	(5.74)	(50.4)	(>1e6)
14. Methyl Chloride	CH_3Cl	1.47	1.17-1.85	± 23	1.52	51.2	150300
		(1.45)	(1.02-2.05)	(± 35)	(1.49)	(52.9)	(105500)
15. Methyl Bromide	CH_3Br	1.65	1.34-2.01	± 20	1.72	36.6	>1e6
		(1.70)	(1.32-2.18)	(± 25)	(1.78)	(38.2)	(>1e6)
16. HCFC−22	$CHClF_2$	12.2	10.0-14.9	± 20	13.0	235.4	3175
		(12.0)	(9.00-16.0)	(± 29)	(12.7)	(232)	(4900)
17. HCFC−141b	CH_3CCl_2F	9.2	7.6-11.1	± 19	10.3	84.2	>1e6
		(9.20)	(6.51-12.8)	(± 34)	(10.3)	(84.3)	(>1e6)
18. HCFC−142b	CH_3CClF_2	17.5	12.9-23.6	± 31	19.0	233.3	2843
		(17.5)	(11.2-27.0)	(± 45)	(19.0)	(226.1)	(3952)
19. HFC−23	CHF_3	223.8	159.4-313.3	± 34	238.8	4183	23980
		(226.4)	(160.2-319.5)	(± 35)	(238.8)	(4687)	(60230)
20. HFC−32	CH_2F_2	5.21	4.24-6.37	± 20	5.41	142.2	5313
		(5.21)	(3.54-7.60)	(± 39)	(5.41)	(142)	(6308)
21. HFC−125	CHF_2CF_3	30.6	23.7-39.5	± 26	32.4	593.3	9129
		(29.3)	(18.6-46.0)	(± 47)	(32.2)	(352.6)	(5454)
22. HFC−134a	CH_2FCF_3	13.4	10.4-17.3	± 26	14.1	290.9	4295
		(13.6)	(9.80-18.6)	(± 32)	(14.3)	(296.4)	(6772)
23. HFC−143a	CF_3CH_3	51.0	38.9-65.7	± 26	56.4	672.1	2555
		(50.1)	(38.0-65.4)	(± 27)	(54.4)	(677.7)	(8517)
24. HFC−152a	CH_3CHF_2	1.45	1.26-1.67	± 14	1.50	47.6	46700
		(1.45)	(1.21-1.73)	(± 18)	(1.50)	(48.1)	(48950)
25. HFC−227ea	CF_3CHFCF_3	35.6	25.6-49.4	± 33	37.7	673.4	9954
		(42.3)	(29.0-61.3)	(± 38)	(44.6)	(899.3)	(15910)
26. HFC−245fa	$CHF_2CH_2CF_3$	7.73	5.44-10.9	± 35	8.13	162.1	4414
		(7.79)	(4.85-12.4)	(± 48)	(8.16)	(178.8)	(6672)
27. Nitrogen Trifluoride	NF_3	569.2	493.8-679.2	± 16	84150	740.7	2531
		(1588)	(1031-2951)	(± 60)	(84150)	(1804)	(15680)

* Model input kinetic and photochemical parameters from the present SPARC evaluation at the 2σ uncertainty limits. The calculated values obtained using the JPL10-6 evaluation recommended input parameters are given in parentheses.

** Using interactive model calculation; % range in lifetime is not symmetric; the value given is a rounded-off average.

Table 3.8. The range in global annually averaged atmospheric lifetimes obtained using a 2-D model for 2000 steady-state conditions with perturbations in the O_3 (±4%) and O_2 (±10 and ±20%) UV absorption cross sections.

Compound	Chemical Formula	Base Lifetime (yrs) *	O_3 Cross-Section Perturbation	O_2 Cross-Section Perturbation (±10%)			O_2 Cross-Section Perturbation (±20%)			Perturbation Lifetime Range / (% from Base) **
				All λ	<204 nm	>204 nm	All λ	<204 nm	>204 nm	
1. CFC-11	CCl_3F	60.2	59.9–60.5 (-0.5, +0.5)	54.2–65.7 (-10, +9.1)	55.8–64.1 (-7.3, +6.5)	58.3–61.7 (-3.2, +2.5)	47.8–70.8 (-21, +18)	50.8–67.3 (-16, +12)	55.8–62.9 (-7.3, +4.5)	49.8–67.8 (-17, +13)
2. CFC-12	CCl_2F_2	109.5	109–110 (-0.4, +0.4)	103–115 (-5.9, +5)	104–114 (-5, +4.1)	108–111 (-1.4, +1.4)	96.1–121 (-12, +11)	99–118 (-9.6, +7.7)	106–112 (-3.2, +2.3)	98.3–118 (-10, +8)
3. CFC-113	CCl_2FCClF_2	93.6	93.4–93.7 (-0.2, +0.1)	87.5–99 (-6.5, +5.8)	89.1–97.6 (-4.8, +4.3)	91.8–95 (-1.9, +1.5)	81.1–104 (-13, +11)	84–101 (-10, +7.9)	89.7–96.2 (-4.2, +2.8)	83.2–101 (-11, +8)
4. CFC-114	$CClF_2CClF_2$	199.7	200–200 (0, 0)	190–208 (-4.9, +4.2)	193–206 (-3.4, +3.2)	197–202 (-1.4, +1.2)	180–216 (-9.9, +8.2)	186–211 (-6.9, +5.7)	194–204 (-2.9, +2.2)	184–212 (-8, +6)
5. CFC-115	CF_3CClF_2	539.9	540–539 (0, -0.2)	525–552 (-2.7, +2.2)	530–548 (-1.8, +1.5)	535–544 (-0.9, +0.8)	509–563 (-5.7, +4.3)	519–555 (-3.9, +2.8)	530–548 (-1.8, +1.5)	517–557 (-4, +3)
6. Carbon Tetrachloride	CCl_4	48.7	48.4–49 (-0.6, +0.6)	42.9–54.1 (-12, +11)	45.1–51.8 (-7.4, +6.4)	46.1–50.8 (-5.3, +4.3)	36.9–59.2 (-24, +22)	41–54.4 (-16, +12)	42.8–52.4 (-12, +7.6)	39.0–55.5 (-20, +14)
7. Nitrous Oxide	N_2O	125.2	125–125 (0, 0)	118–131 (-5.7, +4.6)	120–129 (-4.1, +3.4)	123–127 (-1.7, +1.4)	111–138 (-11, +10)	115–133 (-8.1, +6.2)	120–129 (-4.1, +3)	114–134 (-9, +7)
8. Halon-1202	CBr_2F_2	2.54	2.52–2.57 (-0.8, +1.2)	2.50–2.57 (-1.6, +1.2)	2.50–2.57 (-1.6, +1.2)	2.50–2.54 (-1.6, 0)	2.45–2.59 (-3.5, +2)	2.47–2.61 (-2.7, +2.7)	2.53–2.53 (-0.4, -0.4)	2.46–2.61 (-3, +3)
9. Halon-1211	$CBrClF_2$	16.3	16.2–16.5 (-0.6, +1.2)	15.2–17.2 (-6.7, +5.5)	15.7–16.9 (-3.7, +3.7)	15.8–16.7 (-3.1, +2.5)	13.9–18 (-15, +10)	14.8–17.4 (-9.2, +6.7)	15.2–16.9 -6.7, +3.7)	14.4–17.5 (-12, +7)
10. Halon-1301	$CBrF_3$	77.4	77.2–77.7 (-0.3, +0.4)	71.5–82.7 (-7.7, +6.8)	74.1–80.4 (-4.3, +3.9)	74.6–79.8 (-3.6, +3.1)	65.2–87.7 (-16, +13)	70.2–82.8 (-9.4, +7)	71.2–81.7 (-8, +5.6)	67.9–84.3 (-12, +9)
11. Halon-2402	$CBrF_2CBrF_2$	27.8	27.6–28.1 (-0.7, +1.1)	24.8–30.6 (-11, +10)	26–29.4 (-6.5, +5.7)	26.4–28.9 (-5, +4)	21.5–33 (-23, +19)	23.8–30.7 (-14, +10)	24.6–29.7 (-12, +6.8)	22.7–31.2 (-18, +12)
12. Nitrogen Trifluoride	NF_3	569.2	569–569 (0, 0)	546–590 (-4.1, +3.7)	552–585 (-3, +2.8)	563–574 (-1.1, +0.8)	520–609 (-8.6, +7)	532–599 (-6.5, +5.2)	556–579 (-2.3, +1.7)	530–601 (-7, +6)

* The base lifetimes are from Tables 3.6 and 3.7.

** The percent change from the base lifetime is given in parentheses. The overall perturbation lifetime range recommended here, due to the O_3 and O_2 perturbations only, combines the uncertainties from the O_3 and O_2 (±20%) cross-section perturbations using the above and below 204 nm results (see text for details).

3.8 References

Addison, M. C., R. J. Donovan, and J. Garraway, Reactions of $O(^1D)$ and $O(^3P)$ with halogenomethanes, *Faraday Disc. Chem. Soc., 67*, 286-296, 1979.

Amimoto, S. T., A. P. Force, and J. R. Wiesenfeld, Ozone photochemistry: Production and deactivation of $O(2^1D_2)$ following photolysis at 248 nm, *Chem. Phys. Lett., 60*, 40-43, 1978.

Anderson, D. E., Jr., and R. R. Meier, Effects of anisotropic multiple scattering on solar radiation in the troposphere and stratosphere, *Appl. Opt., 18*, 1955-1960, 1979.

Atkinson, R., D. A. Hansen, and J. N. Pitts, Jr., Rate constants for the reaction of OH radicals with CHF_2Cl, CF_2Cl_2, $CFCl_3$, and H_2 over the temperature range 297-434 K, *J. Chem. Phys., 63*, 1703-1706, 1975.

Atkinson, R., G. M. Breuer, J. N. Pitts, Jr., and H. L. Sandoval, Tropospheric and stratospheric sinks for halocarbons: Photooxidation, $O(^1D)$ atom, and OH radical reactions, *J. Geophys. Res., 81*, 5765-5770, 1976.

Atkinson, R., D. L. Baulch, R. A. Cox, J. N. Crowley, R. F. Hampson, R. G. Hynes, M. E. Jenkin, M. J. Rossi, J. Troe, and T. J. Wallington, Evaluated kinetic and photochemical data for atmospheric chemistry: Volume IV - gas phase reactions of organic halogen species, *Atmos. Chem. Phys., 8*, 4141-4496, 2008.

Baasandorj, M., K. J. Feierabend, and J. B. Burkholder, Rate coefficients and ClO radical yields in the reaction of $O(^1D)$ with $CClF_2CCl_2F$, CCl_3CF_3, $CClF_2CClF_2$, and CCl_2FCF_3, *Int. J. Chem. Kinet., 43*, 1-9, 2011.

Baasandorj, M., B. D. Hall, and J. B. Burkholder, Rate coefficients for the reaction of $O(^1D)$ with the atmospherically long-lived greenhouse gases NF_3, SF_5CF_3, CHF_3, C_2F_6, c-C_4F_8, n-C_5F_{12}, and n-C_6F_{14}, *Atmos. Chem. Phys., 12*, 11753-11764, 2012.

Baasandorj, M., E. L. Fleming, C. H. Jackman, and J. B. Burkholder, $O(^1D)$ kinetic study of key ozone depleting substances and greenhouse gases, *J. Phys. Chem. A*, dx.doi.org/10.1021/jp310910f, 2013.

Beichert, P., J. L. Wingen, R. Vogt, M. J. Ezell, M. Ragains, R. Neavyn, and B. J. Finlayson-Pitts, Rate constants for the reactions of chlorine atoms with some simple alkanes at 298 K: Measurement of a self-consistent set using both absolute and relative rate methods, *J. Phys. Chem., 99*, 13156-13162, 1995.

Biermann, H. W., C. Zetzsch, and F. Stuhl, Rate constant for reaction of OH with N_2O at 298 K, *Ber. Bunsenges. Phys. Chem., 80*, 909-911, 1976.

Blitz, M. A., T. J. Dillon, D. E. Heard, M. J. Pilling, and I. D. Trought, Laser induced fluorescence studies of the reactions of $O(^1D_2)$ with N_2, O_2, N_2O, CH_4, H_2, CO_2, Ar, Kr and n-C_4H_{10}, *Phys. Chem. Chem. Phys., 6*, 2162-2171, 2004.

Bryukov, M. G., I. R. Slagle, and V. D. Knyazev, Kinetics of reactions of Cl atoms with methane and chlorinated methanes *J. Phys. Chem. A, 106*, 10532-10542, 2002.

Burkholder, J. B., R. R. Wilson, T. Gierczak, R. Talukdar, S. A. McKeen, J. J. Orlando, G. L. Vaghjiani, and A. R. Ravishankara, Atmospheric fate of CF_3Br, CF_2Br_2, CF_2ClBr, and CF_2BrCF_2Br, *J. Geophys. Res., 96*, 5025-5043, 1991.

Cavalli, F., M. Glasius, J. Hjorth, B. Rindone, and N. R. Jensen, Atmospheric lifetimes, infrared spectra and degradation products of a series of hydrofluoroethers, *Atmos. Environ., 32*, 3767-3773, 1998.

Chang, J. S., and F. Kaufman, Kinetics of the reactions of hydroxyl radicals with some halocarbons: $CHFCl_2$, CHF_2Cl, CH_3CCl_3, C_2HCl_3, and C_2Cl_4, *J. Chem. Phys., 66*, 4989-4994, 1977a.

Chang, J. S., and F. Kaufman, Upper limits of the rate constants for the reactions of $CFCl_3$(F-ll), CF_2C1_2(F-12), and N_2O with OH. Estimates of corresponding lower limits to their tropospheric lifetimes, *Geophys. Res. Lett., 4*, 192-194, 1977b.

Chen, J., V. Young, and H. Niki, Kinetic and mechanistic studies for reactions of $CF_3CH_2CHF_2$ (HFC-245fa) initiated by H-atom abstraction using atomic chlorine, *J. Phys. Chem. A, 101*, 2648-2653, 1997.

Chichinin, A., S. Teton, G. LeBras, and G. Poulet, Kinetic investigation of the OH + CH_3Br reaction between 248 and 390 K, *J. Atmos. Chem., 18*, 239-245, 1994.

Clyne, M. A. A., and P. M. Holt, Reaction kinetics involving ground $X^2\Pi$ and excited $A^2\Sigma^+$ hydroxyl radicals. Part 2. Rate constants for reactions of OH $X^2\Pi$ with halogenomethanes and halogenoethanes, *J. Chem. Soc. Faraday Trans. 2, 75*, 582-591, 1979.

Cronkhite, J. M., and P. H. Wine, Branching ratios for BrO production from reactions of $O(^1D)$ with HBr, CF_3Br, CH_3Br, CF_2ClBr, and CF_2HBr, *Int. J. Chem. Kinet.*, 30, 555-563, 1998.

Curtiss, L. A., P. C. Redfern, K. Raghavachari, and J. A. Pople, Gaussian-3X (G3X) theory: Use of improved geometries, zero-point energies, and Hartree-Fock basis sets, *J. Chem. Phys., 114*, 108-117, 2001.

Davidson, J. A., H. I. Schiff, T. J. Brown, and C. J. Howard, Temperature dependence of the rate constants for reactions of $O(^1D)$ atoms with a number of halocarbons, *J. Chem. Phys., 69*, 4277-4279, 1978.

DeMore, W. B., Rate constants for the reactions of OH with HFC-134a (CF_3CH_2F) and HFC-134 (CHF_2CHF_2), *Geophys. Res. Lett., 20*, 1359-1362, 1993.

Dillon, T. J., A. Horowitz, and J. N. Crowley, Cross-sections and quantum yields for the atmospheric photolysis of the potent greenhouse gas nitrogen trifluoride, *Atmos. Env., 44*, 1186-1191, 2010.

Dillon, T. J., L. Vereecken, A. Horowitz, V. Khamaganov, J. N. Crowley, and J. Lelieveld, Removal of the potent greenhouse gas NF_3 by reactions with the atmospheric oxidants $O(^1D)$, OH and O_3, *Phys. Chem. Chem. Phys., 13*, 18600-18608, 2011.

Fang, T. D., P. H. Taylor, and B. Dellinger, Absolute rate measurements of the reaction of OH radicals with HCFC-21 ($CHFCl_2$) and HCFC-22 (CHF_2Cl) over an extended temperature range, *J. Phys. Chem., 100*, 4048-4054, 1996.

Feierabend, K. J., D. K. Papanastasiou, and J. B. Burkholder, ClO radical yields in the reaction of $O(^1D)$ with Cl_2, HCl, chloromethanes and chlorofluoromethanes, *J. Phys. Chem. A, 114*, 12052-12061, 2010.

Fleming, E. L., C. H. Jackman, R. S. Stolarski, and A. R. Douglas, A model study of the impact of source gas changes on the stratosphere for 1850-2100, *Atmos. Chem. Phys., 11*, 8515-8541, 2011.

Force, A. P., and J. R. Wiesenfeld, Collisional deactivation of $O(^1D_2)$ by the halomethanes. Direct determination of reaction efficiency, *J. Phys. Chem.*, *85*, 782-785, 1981.

Gillotay, D., and P. C. Simon, Ultraviolet absorption spectrum of trifluoro-bromo-methane, difluoro-dibromo-methane and difluoro-bromo-chloro-methane in the vapor phase, *J. Atmos. Chem.*, *8*, 41-62, 1989.

Gillotay, D., and P. C. Simon, Temperature-dependence of ultraviolet absorption cross-sections of alternative chlorofluoroethanes, *J. Atmos. Chem.*, *12*, 269-285, 1991.

Green, R. G., and R. P. Wayne, Relative rate constants for the reactions of $O(^1D)$ atoms with fluorochlorocarbons and with N_2O, *J. Photochem.*, *6*, 371-374, 1976/77.

Greenblatt, G. D, and A. R. Ravishankara, Laboratory studies on the stratospheric NO_x production rate, *J. Geophys. Res.*, *95*, 3539-3547, 1990.

Grooß, J.-U., and R. Müller, Do cosmic-ray-driven electron-induced reactions impact stratospheric ozone depletion and global climate change?, *Atmos. Environ.*, *45*, 3508-3514, 2011.

Gurvich, L. V., I. V. Veyts, and C. B. Alcock, *Thermodynamic Properties of Individual Substances*, Fourth ed., Hemisphere Pub. Co., New York, 1989.

Handwerk, V., and R. Zellner, Kinetics of the reactions of OH radicals with some halocarbons ($CHClF_2$, CH_2ClF, CH_2ClCF_3, CH_3CClF_2, CH_3CHF_2) in the temperature range 260-370 K, *Ber. Bunsenges. Phys. Chem.*, *82*, 1161-1166, 1978.

Harris, N. R. P., J. C. Farman, and D. W. Fahey, Comment on "Effects of cosmic rays on atmospheric chlorofluorocarbon dissociation and ozone depletion", *Phys. Rev. Lett.*, *89*, 219801, 2002.

Harrison, H., Climatic Impact Assessment Program, 1975.

Heidner, R. F. I., and D. Husain, Electronically excited oxygen atoms, $O(2^1D_2)$. A time-resolved study of the collisional quenching by the gases H_2, D_2, NO, N_2O, NO_2, CH_4, and C_3O_2. Using atomic absorption spectroscopy in the vacuum ultraviolet, *Int. J. Chem. Kinet.*, *5*, 819-831, 1973.

Herndon, S. C., T. Gierczak, R. K. Talukdar, and A. R. Ravishankara, Kinetics of the reactions of OH with several alkyl halides, *Phys. Chem. Chem. Phys.*, *3*, 4529-4535, 2001.

Howard, C. J., and K. M. Evenson, Rate constants for the reactions of OH with ethane and some halogen substituted ethanes at 296 K, *J. Chem. Phys.*, *64*, 4303-4306, 1976.

Hsu, K. J., and W. B. DeMore, Rate constants for the reactions of OH with CH_3Cl, CH_2Cl_2, $CHCl_3$, and CH_3Br, *Geophys. Res. Lett.*, *21*, 805-808, 1994.

Hsu, K. J., and W. B. DeMore, Rate constants and temperature dependences for the reactions of hydroxyl radical with several halogenated methanes, ethanes, and propanes by relative rate measurements, *J. Phys. Chem.*, *99*, 1235-1244, 1995.

Hubrich, C., and F. Stuhl, The ultraviolet absorption of some halogenated methanes and ethanes of atmospheric interest, *J. Photochem.*, *12*, 93-107, 1980.

Jeong, K.-M., and F. Kaufman, Kinetics of the reaction of hydroxyl radical with methane and with nine Cl- and F-substituted methanes. I. Experimental results, comparisons, and applications, *J. Phys. Chem.*, *86*, 1808-1815, 1982.

Kaiser, E. W., Relative rate constants for reactions of HFC 152a, 143, 143a, 134a, and HCFC 124 with F or Cl atoms and for CF_2CH_3, CF_2HCH_2, and CF_3CFH radicals with F_2, Cl_2, and O_2, *Int. J. Chem. Kinet., 25*, 667-680, 1993.

Kaye, J. A., S. A. Penkett, and F. M. Ormond, Report on concentrations, lifetimes, and trends of CFCs, halons, and related species, NASA Reference Publication 1339, 1994.

Keller-Rudek, H., and G. K. Moortgat, MPI-Mainz-UV-VIS Spectral Atlas of Gaseous Molecules, http://www.atmosphere.mpg.de/spectral-atlas-mainz.

Kozlov, S. N., V. L. Orkin, and M. J. Kurylo, An investigation of the reactivity of OH with fluoroethanes: CH_3CH_2F (HFC-161), CH_2FCH_2F (HFC-152), and CH_3CHF_2 (HFC-152a), *J. Phys. Chem. A, 107*, 2239-2246, 2003.

Lancar, I., G. Le Bras, and G. Poulet, Oxidation of CH_3CCl_3 and CH_3CFCl_2 in the atmosphere - Kinetic study of OH reactions, *J. Chim. Physique, 90*, 1897-1908, 1993.

Louis, F., A. Talhaoui, J. P. Sawerysyn, M.-T. Rayez, and J.-C. Rayez, Rate coefficients for the gas phase reactions of CF_3CH_2F (HFC-134a) with chlorine and fluorine atoms: Experimental and ab initio theoretical studies, *J. Phys. Chem. A, 101*, 8503-8507, 1997.

Lu, Q. B., Correlation between cosmic rays and ozone depletion, *Phys. Rev. Lett., 102*, 118501, 2009.

Lu, Q. B., Cosmic-ray-driven electron-induced reactions of halogenated molecules adsorbed on ice surfaces: Implications for atmospheric ozone depletion and global climate change, *Phys. Rep., 487*, 141-167, 2010.

Lu, Q. B., and L. Sanche, Effects of cosmic rays on atmospheric chlorofluorocarbon dissociation and ozone depletion, *Phys. Rev. Lett., 87*, 078501, 2001.

Makeev, G. N., V. F. Sinyanskii, and B. M. Smirnov, Absorption spectra of certain fluorides in the near ultraviolet region, *Doklady Phys. Chem., 222*, 452-455, 1975.

Manning, R., and M. J. Kurylo, Flash photolysis resonance fluorescence investigation of the temperature dependencies of the reactions of $Cl(^2P)$ atoms with CH_4, CH_3Cl, CH_3F, CH_3F, and C_2H_6, *J. Phys. Chem., 81*, 291-296, 1977.

Matsumi, Y., K. Tonokura, Y. Inagaki, and M. Kawasaki, Isotopic branching ratios and translational energy release of H and D atoms in reaction of $O(^1D)$ atoms with alkanes and alkyl chlorides, *J. Phys. Chem., 97*, 6816-6821, 1993.

Mellouki, A., R. K. Talukdar, A. -M. Schmoltner, T. Gierczak, M. J. Mills, S. Solomon, and A. R. Ravishankara, Atmospheric lifetimes and ozone depletion potentials of methyl bromide (CH_3Br) and dibromomethane (CH_2Br_2), *Geophys. Res. Lett., 19*, 2059-2062, 1992.

Minschwaner, K., L. Hoffmann, A. Brown, M. Riese, R. Müller, and P. F. Bernath, Stratospheric loss and atmospheric lifetimes of CFC-11 and CFC-12 derived from satellite observations, *Atmos. Chem. Phys. Discuss., 12*, 28733-28764, 2012.

Møgelberg, T. E., J. Sehested, M. Bilde, T. J. Wallington, and O. J. Nielsen, Atmospheric chemistry of CF_3CFHCF_3 (HFC-227ea): Spectrokinetic investigation of the $CF_3CFO_2CF_3$ radical, its reactions with NO and NO_2, and fate of the CF_3CFOCF_3 radicals, *J. Phys. Chem., 100*, 8882-8889, 1996.

Molina, L. T., P. J. Wooldridge, and M. J. Molina, Atmospheric reactions and ultraviolet and infrared absorptivities of nitrogen trifluoride, *Geophys. Res. Lett., 22,* 1873-1876, 1995.

Müller, R., Impact of cosmic rays on stratospheric chlorine chemistry and ozone depletion, *Phys. Rev. Lett., 91,* 058502, 2003.

Müller, R., and J. U. Grooß, Does cosmic-ray-induced heterogeneous chemistry influence stratospheric polar ozone loss?, *Phys. Rev. Lett., 103,* 228501, 2009.

Nayak, A. K., T. J. Buckley, M. J. Kurylo, and A. Fahr, Temperature dependence of the gas and liquid phase ultraviolet absorption cross sections of HCFC-123 (CF_3CHCl_2) and HCFC-142b (CH_3CF_2Cl), *J. Geophys. Res.*, 101, 9055-9062, 1996.

Nelson, D. D. J., M. S. Zahniser, and C. E. Kolb, OH reaction kinetics and atmospheric lifetimes of CF_3CFHCF_3 and CF_3CH_2Br, *Geophys. Res. Lett., 20,* 197-200, 1993.

Nielsen, O. J., T. Ellermann, E. Bartkiewicz, T. J. Wallington, and M. D. Hurley, UV absorption spectra, kinetics and mechanisms of the self-reaction of CHF_2O_2 radicals in the gas phase at 298 K, *Chem. Phys. Lett., 192,* 82-88, 1992.

Nielsen, O. J., E. Gamborg, J. Sehested, T. J. Wallington, and M. D. Hurley, Atmospheric chemistry of HFC-143a: Spectrokinetic investigation of the $CF_3CH_2O_2$ radical, its reactions with NO and NO_2, and the fate of CF_3CH_2O, *J. Phys. Chem., 98,* 9518-9525, 1994.

Nilsson, E. J. K., M. S. Johnson, O. J. Nielsen, E. W. Kaiser, and T. J. Wallington, Kinetics of the gas-phase reactions of chlorine atoms with CH_2F_2, CH_3CCl_3, and CF_3CFH_2 over the temperature range 253-553 K, *Int. J. Chem. Kinet., 41,* 401-406, 2009.

Nilsson, E. J. K., V. F. Andersen, O. J. Nielsen, and M. S. Johnson, Rate coefficients for the chemical reactions of CH_2F_2, $CHClF_2$, CH_2FCF_3 and CH_3CCl_3 with $O(^1D)$ at 298 K. *Chem. Phys. Lett., 554,* 27-32, 2012.

Orkin, V. L., and V. G. Khamaganov, Determination of rate constants for reactions of some hydrohaloalkanes with OH radicals and their atmospheric lifetimes, *J. Atmos. Chem., 16,* 157-167, 1993.

Orkin, V. L., V. G. Khamaganov, E. E. Kasimovskaya, and A. G. Guschin, Photochemical properties of some Cl-containing halogenated alkanes, *submitted to J. Phys. Chem.*, 2013.

Orlando, J. J., Temperature dependence of the rate coefficients for the reaction of chlorine atoms with chloromethanes, *Int. J. Chem. Kinet., 31,* 515-524, 1999.

Orlando, J. J., J. B. Burkholder, S. A. McKeen, and A. R. Ravishankara, Atmospheric fate of several hydrofluoroethanes and hydrochloroethanes: 2. UV absorption cross sections and atmospheric lifetimes, *J. Geophys. Res., 96,* 5013-5023, 1991.

Papanastasiou, D., N. Rontu Carlon, J. A. Neuman, E. L. Fleming, C. H. Jackman, and J. B. Burkholder, Revised UV absorption cross sections of CF_2Br_2, CF_2ClBr, and CF_2BrCF_2Br and ozone depletion potentials, *Geophys. Res. Lett., 40,* doi: 10.1002/grl.50121, 2013.

Papadimitriou, V. C., M. McGillen, E. L. Fleming, C. H. Jackman, and J. B. Burkholder, NF_3: UV absorption spectrum temperature dependence and the atmospheric lifetime implications, *Geophys. Res. Lett., 40,* doi: 10.1002/grl.50120, 2013.

Paraskevopoulos, G., D. L. Singleton, and R. S. Irwin, Rates of OH radical reactions. 8. Reactions with CH_2FCl, CHF_2Cl, $CHFCl_2$, CH_3CF_2Cl, CH_3Cl, and C_2H_5Cl at 297 K, *J. Phys. Chem., 85*, 561-564, 1981.

Patra, P. K., and M. S. Santhanam, Comment on "Effects of cosmic rays on atmospheric chlorofluorocarbon dissociation and ozone depletion", *Phys. Rev. Lett., 89*, 219803, 2002.

Platz, J., O. J. Nielsen, J. Sehested, and T. J. Wallington, Atmospheric chemistry of 1,1,1-trichloroethane: UV spectra and self-reaction kinetics of CCl_3CH_2 and $CCl_3CH_2O_2$ radicals, kinetics of the reactions of the $CCl_3CH_2O_2$ radical with NO and NO_2, and the fate of the alkoxy radical CCl_3CH_2O, *J. Phys. Chem., 99*, 6570-6579, 1995.

Rontu Carlon, N., D. K. Papanastasiou, E. L. Fleming, C. H. Jackman, P. A. Newman, and J. B. Burkholder, UV absorption cross sections of nitrous oxide (N_2O) and carbon tetrachloride (CCl_4) between 210 and 350 K and the atmospheric implications, *Atmos. Chem. Phys., 10*, 6137-6149, 2010.

Sander, S. P., J. Abbatt, J. R. Barker, J. B. Burkholder, R. R. Friedl, D. M. Golden, R. E. Huie, C. E. Kolb, M. J. Kurylo, G. K. Moortgat, V. L. Orkin, and P. H. Wine, *Chemical Kinetics and Photochemical Data for Use in Atmospheric Studies, Evaluation Number 17, JPL Publication 10-6,* Jet Propulsion Laboratory, California Institute of Technology 2011.

Sarzyński, D., A. A. Gola, A. Dryś, and J. T. Jodkowski, Kinetic study of the reaction of chlorine atoms with chloromethane in the gas phase, *Chem. Phys. Lett., 476*, 138-142, 2009.

Simon, P. C., D. Gillotay, N. Vanlaethem-Meuree, and J. Wisemberg, Temperature dependence of ultraviolet absorption cross-sections of chlorofluoroethanes, *Annales Geophysicae, 6*, 239-248, 1988a.

Simon, P. C., D. Gillotay, N. Vanlaethem-Meuree, and J. Wisemberg, Ultraviolet absorption cross-sections of chloro and chlorofluoro-methanes at stratospheric temperatures, *J. Atmos. Chem., 7*, 107-135, 1988b.

Spivakovsky, C. M., J. A. Logan, S. A. Montzka, Y. J. Balkanski, M. Foreman-Fowler, D. B. J. Jones, L. W. Horowitz, A. C. Fusco, C. A. M. Brenninkmeijer, M. J. Prather, S. C. Wofsy, and M. B. McElroy, Three-dimensional climatological distribution of tropospheric OH: Update and evaluation, *J. Geophys. Res., 105*, 8931-8980, 2000.

Staudinger, J., and P. V. Roberts, A critical compilation of Henry's law constant temperature dependence relations for organic compounds in dilute aqueous solutions, *Chemosphere, 44*, 561-576, 2001.

Swartz, W. H., S. A. Lloyd, T. L. Kusterer, D. E. Anderson, C. T. McElroy, and C. Midwinter, A sensitivity study of photolysis rate coefficients during POLARIS, *J. Geophys. Res., 104*, 26725-26735, 1999.

Talhaoui, A., F. Louis, P. Devolder, B. Meriaux, J. P. Sawerysyn, and M. T. Rayez, Rate coefficients of the reactions of chlorine atoms with haloethanes of type $CH_3CCl_{3-x}F_x$ (x = 0, 1, and 2): Experimental and ab initio theoretical studies, *J. Phys. Chem., 100*, 13531-13538, 1996.

Talukdar, R., A. Mellouki, T. Gierczak, J. B. Burkholder, S. A. McKeen, and A. R. Ravishankara, Atmospheric fate of CF_2H_2, CH_3CF_3, CHF_2CF_3, and CH_3CFCl_2: Rate coefficients for reactions with OH and UV absorption cross sections of CH_3CFCl_2, *J. Phys. Chem.*, *95*, 5815-5821, 1991.

Tokuhashi, K., L. Chen, S. Kutsuna, T. Uchimaru, M. Sugie, and A. Sekiya, Environmental assessment of CFC alternatives: Rate constants for the reactions of OH radicals with fluorinated compounds, *J. Fluor. Chem.*, *125*, 1801-1807, 2004.

Tschuikow-Roux, E., T. Yano, and J. Niedzielski, Reactions of ground state chlorine atoms with fluorinated methanes and ethanes, *J. Chem. Phys.*, *82*, 65-74, 1985.

Tuazon, E. C., R. Atkinson, and S. B. Corchnoy, Rate constants for the gas-phase reactions of Cl atoms with a series of hydrofluorocarbons and hydrochlorofluorocarbons at 298 ± 2 K, *Int. J. Chem. Kinet.*, *24*, 639-648, 1992.

Vranckx, S., J. Peeters, and S. Carl, A temperature dependence kinetic study of $O(^1D) + CH_4$: Overall rate coefficient and product yields, *Phys. Chem. Chem. Phys.*, *10*, 5714-5722, 2008.

Wallington, T. J., J. M. Andino, J. C. Ball, and S. M. Japar, Fourier transform infrared studies of the reaction of Cl atoms with PAN, PPN, CH_3OOH, HCOOH, CH_3COCH_3 and $CH_3COC_2H_5$ at 295 ± 2 K, *J. Atmos. Chem.*, *10*, 301-313, 1990.

Wallington, T. J., and M. D. Hurley, A kinetic study of the reaction of chlorine atoms with CF_3CHCI_2, CF_3CH_2F, $CFCl_2CH_3$, CF_2ClCH_3, CHF_2CH_3, CH_3D, CH_2D_2, CHD_3, CD_4, and CD_3Cl at 295 ± 2 K, *Chem. Phys. Lett.*, *189*, 437-442, 1992.

Wallington, T. J., M. D. Hurley, O. J. Nielsen, and M. P. S. Andersen, Atmospheric chemistry of $CF_3CFHCF_2OCF_3$ and $CF_3CFHCF_2OCF_2H$: Reaction with Cl atoms and OH radicals, degradation mechanism, and global warming potentials, *J. Phys. Chem. A*, *108*, 11333-11338, 2004.

Warren, R., T. Gierczak, and A. R. Ravishankara, A study of $O(^1D)$ reactions with CFC substitutes, *Chem. Phys. Lett.*, *183*, 403-409, 1991.

Warren, R. F., and A. R. Ravishankara, Kinetics of $Cl(^2P)$ reactions with CF_3CHCl_2, CF_3CHFCl, and CH_3CFCl_2, *Int. J. Chem. Kinet.*, *25*, 833-844, 1993.

Watson, R. T., G. Machado, B. Conaway, S. Wagner, and D. D. Davis, A temperature dependent kinetics study of the reaction of OH with CH_2ClF, $CHCl_2F$, $CHClF_2$, CH_3CCl_3, CH_3CF_2Cl, and $CF_2ClCFCl_2$, *J. Phys. Chem.*, *81*, 256-262, 1977.

Wine, P. H., and A. R. Ravishankara, Kinetics of $O(^1D)$ interactions with the atmospheric gases N_2, N_2O, H_2O, H_2, CO_2, and O_3, *Chem. Phys. Lett.*, *77*, 103-109, 1981.

WMO (World Meteorological Organization), *Scientific Assessment of Ozone Depletion: 2006*, *Global Ozone Research and Monitoring Project-Report* No. 50, 2007.

WMO (World Meteorological Organization), *Scientific Assessment of Ozone Depletion: 2010*, *Global Ozone Research and Monitoring Project-Report* No. 52, 2011.

Yano, T., and E. Tschuikow-Roux, Competitive photochlorination of the fluoroethanes CH_3CHF_2, CH_2FCH_2F and CHF_2CHF_2, *J. Photochem.*, *32*, 25-37, 1986.

Young, C. J., M. D. Hurley, T. J. Wallington, and S. A. Mabury, Atmospheric chemistry of CF_3CF_2H and $CF_3CF_2CF_2CF_2H$: Kinetics and products of gas-phase reactions with Cl atoms and OH radicals, infrared spectra, and formation of perfluorocarboxylic acids, *Chem. Phys. Lett.*, *473*, 251-256, 2009.

Zellner, R., G. Bednarek, A. Hoffmann, J. P. Kohlmann, V. Mors, and H. Saathoff, Rate and mechanism of the atmospheric degradation of 2 H-heptafluoropropane (HFC-227), *Ber. Bunsenges. Phys. Chem.*, *98*, 141-146, 1994.

Zhang, Z., S. Padmaja, R. D. Saini, R. E. Huie, and M. J. Kurylo, Reactions of hydroxyl radicals with several hydrofluorocarbons: The temperature dependencies of the rate constants for $CHF_2CF_2CH_2F$ (HFC-245ca), $CF_3CHFCHF_2$ (HFC-236ea), CF_3CHFCF_3 (HFC-227ea), and $CF_3CH_2CH_2CF_3$ (HFC-356ffa), *J. Phys. Chem.*, *98*, 4312-4315, 1994.

Zhang, Z., R. D. Saini, M. J. Kurylo, and R. E. Huie, A temperature dependent kinetic study of the reaction of the hydroxyl radical with CH_3Br, *Geophys. Res. Lett.*, *19*, 2413-2416, 1992.

Zhao, Z., P. L. Laine, J. M. Nicovich, and P. H. Wine, Reactive and non-reactive quenching of $O(^1D)$ by the potent greenhouse gases SO_2F_2, NF_3, and SF_5CF_3, *Proc. Nat. Acad. Sci.*, *107*, 6610-6615, 2010.